UNIVERSITÀ DEGLI STUDI DI PADOVA

Dipartimento di Fisica e Astronomia "Galileo Galilei"

Corso di Laurea Magistrale in Fisica

Tesi di Laurea

Flow of a Non-Newtonian Fluid in a porous medium

Relatore

Prof. Marco Baiesi

Correlatore

Dr. Alberto Rosso

Laureando

Federico Lanza

Anno Accademico 2018/2019

UNIVERSITÀ
DEGLI STUDI
DI PADOVA

UNIVERSITÉ
PARIS
SUD

université
PARIS-SACLAY

LPTMS
Laboratoire de Physique Théorique
et Modèles Statistiques

Contents

Introduction

Most of the water used for human consumption is stored in underground porous structures, called aquifers, where it is free to flow if a pressure drop is applied. In 1855 Darcy showed [1] that the mean debit of water is proportional to the stress drop and to the permeability, a constant that depends on the composition of the porous structure and can vary of many order of magnitude.
Predicting the flow of non-Newtonian fluids in similar structures is still a challenging issue due to the interplay between the microscopic disorder and the non-linear rheology. Flows of non-Newtonian fluids through porous medium are of interest in many practical applications in different fields, such as ground reinforcement by cement injection in geologic engineering, hydraulics fracturation for oil extraction [2] or stabilization of bone fractures in biomedical engineering [3]. Some of these fluids, such as mud, heavy oil, foam or emulsions, exhibit a yield stress: they behave like liquid above a critical stress and as solid otherwise. In the last years, experiments [4, 5] and simulations [6] involving yield stress fluid in a porous medium suggested that this system undergoes a continuous phase transition controlled by the applied pressure drop; more specifically, the flow vanishes at a critical value and it is strictly zero for smaller pressure drop, while, above threshold, the flow curve is non-linear. Recently, the geometry of the open channels in two-dimensional structures was numerically studied [7–9], showing that evolves from a single open channel at the threshold to a two dimensional structure that enlarges gradually until a very large pressure drop is reached, above which the Darcy law, and in particular the linearity of the flow, is recovered.

In this thesis we investigate the universal properties at the transition point, confirming the results already known for a two-dimensional system and trying to explore the same system in three dimensions. In particular we're interested in the statistical properties of the length of the first channels that opens just above the pressure threshold. Using

a mapping between this problem and the one of directed polymer in random media, we concentrate mainly on the study of the non-crossing probability of two directed polymer in both two and three dimensions, deriving analytical results and confirming them with numerical simulations. The results found for the three-dimensional system are original.

After a brief historical overview on the Darcy's law, in Chapter 1 we present a lattice model adopted for studying the flow of a fluid in a porous medium, and explain a method, developed specifically for Bingham plastics, to compute the mean flow rate and the geometry of the open channels. To make progress on the statistic of the first channels, we prove a relation between the distribution of the second channel's length, the distribution of the energy gap between the first two channels, and the non-crossing probability of two ground state polymers in disordered media.
An introduction on directed polymers in the continuum limit, both in absence (free case) and in presence (disordered case) of a random environment, opens Chapter 2. We introduce a formula for determining the non-crossing probability between two directed polymers, and we perform analytical calculations explicitly in the free case both in two dimensions, confirming the result already known thanks to the method of images, and in three dimensions. Using a statistical symmetry we show that in two dimension the result valid for the free case holds also in the disordered case.
Chapter 3 focuses on the study of discrete directed polymers on a lattice. We illustrate the algorithms developed for the numerical estimation of the non-crossing probability, both in the free case and the disordered case at zero temperature and for both the dimensions considered, and we present our results.
Chapter 4 is dedicated to the conclusions, giving an outlook on the possible future development of this work, in particular on the statistic of the first-crossing time of directed polymers.

Chapter 1

Darcy's law for non-Newtonian fluids

1.1 The Darcy's law

Henry Darcy (1803 - 1858) was a French engineer specialized in hydraulics that contributed to the construction of bridges, roads and other public works mainly in his hometown, Dijon. In particular, he built there an impressive pressurized water distribution system (see Figure 1.1). The Darcy's aqueduct is considered the first modern aqueduct, and his work became useful to develop hydraulic systems in cities all around the globe; this allowed their inhabitants to supply adequate fresh water, helping them to fight against cholera and other infectious diseases that were widespread at that time due to poor sanitation. After retirement, in 1855 he continued his research in Dijon and realized hydrodynamic experiments that established what has become known as the Darcy's law [1]. In the original experiment (see Figure 1.2) Darcy poured some water into a column of height L entirely filled with sand, and after having applied a pressure P at the top by an hydraulic piston, he measured the amount of outgoing water at the bottom. He showed that the mean debit Q, namely the volume of fluid which comes out per unit time, is proportional to the ratio P/L.
The Darcy's law is not restricted only to water in sands, but is commonly used for oil, natural gas, and most Newtonian fluids embedded in porous structure, as long as the mean flow rate is small enough so that the inertia can be neglected [10–12]. If P is the stress drop applied to the structure and L its size, the Darcy's law says that the mean

Figure 1.1: Monument erected in honour of H. Darcy, situated just above the place where he built the first modern sink in Dijon.

flow rate Q writes

$$Q = \frac{S\kappa}{\mu}\frac{P}{L} \tag{1.1}$$

where S is the cross-sectional area of the structure and μ is the viscosity of the fluid. The proportionality constant κ is called permeability and can vary of many order of magnitude: from the quite large values of fractured rock or gravel to the extremely small permeability of clay. Since it is a macroscopic measure of the interplay between the liquid and the solid at the pore scale, a theoretical prediction of its value requires to solve the Navier-Stokes equations coupled with the no-slip condition at the complex solid interface. The full solution of the problem is computationally costly; nevertheless, a significant simplification is provided by the pore network model [13] shown in Fig. 1.3. There the material is described by a lattice of large voids (the pores) connected by narrow cylindrical tubes (the throats). In the pores the pressure is assumed homogeneous, and the flow occurs in the throats where it can be computed for Newtonian fluids according to the Poiseuille law. The local flow rate q_{ij} in the throat connecting the pores i and j writes then

$$q_{ij} = \sigma_{ij}\Delta p_{ij} \tag{1.2}$$

with the local pressure drop $\Delta p_{ij} = p_i - p_j$, where p_i is the local pressure of the pore i, and the local hydraulic conductivity σ_{ij}; for cylindrical throats of length l and radius r_0

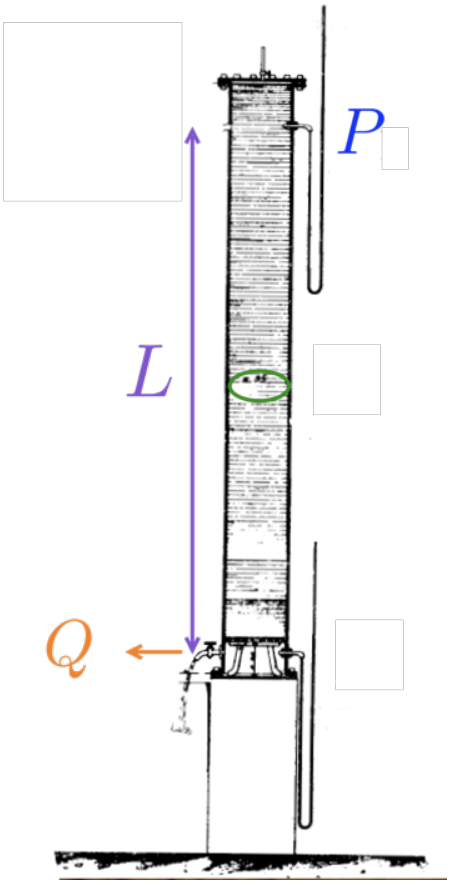

Figure 1.2: Draw of the experiment realized by Darcy in order to prove the linearity between P and Q.

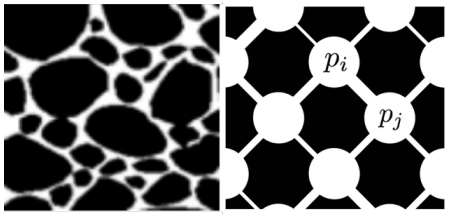

Figure 1.3: Sketch of porous media. Left: realistic porous medium in which the solid structure consists of an assembly of grains (in black) among whom the fluid is free to flow. Right: model of a pore network, in which large voids pores are connected by straight tubes that in general present random radius and length.

$\sigma_{ij} \sim r_0^4/l$. Equation 1.2 should be combined with the Kirchhoff's conservation of the flow at each node $\sum_{j\in n(i)} q_{ij} = 0$, where the sum runs over the set $n(i)$ of neighbours of the node i; this conservation holds for all the N_c nodes of our lattice except the inlet node, where the fluid is injected at pressure P, and the outlet node, where the fluid is evacuated at zero pressure. We define the symmetric matrix A, whose entrance $A_{ij} = \sigma_{ij}$ if the throat (ij) connecting the pores i and j is present in the lattice $\mathcal{L}$ and $A_{ij} = 0$ otherwise:

$$A_{ij} = \begin{cases} \sigma_{ij} \text{ if } (ij) \in \mathcal{L} \\ 0 \text{ else} \end{cases} \tag{1.3}$$

The Kirchhoff condition combined with Eq. 1.2 writes then

$$\sum_{j=i}^{N_c} A_{ij}(p_i - p_j) = 0, \tag{1.4}$$

together with the pressure imposed at the inlet $p_1 = P$ and at the outlet $p_{N_c} = 0$. This system of linear equations can be recast in the matrix form

$$\mathrm{M}\vec{p} = P\vec{v}, \tag{1.5}$$

where

$$\mathrm{M} = \begin{pmatrix} \sum_{j=1}^{N_c} A_{2j} & -A_{23} & \dots & -A_{2,N_c-1} \\ -A_{32} & \sum_{j=1}^{N_c} A_{3j} & \dots & -A_{3,N_c-1} \\ \vdots & \vdots & \ddots & \vdots \\ -A_{N_c-1,2} & -A_{N_c-1,3} & \dots & \sum_{j=1}^{N_c} A_{N_c-1,j} \end{pmatrix}, \ \vec{p} = \begin{pmatrix} p_2 \\ p_3 \\ \vdots \\ p_{N_c-1} \end{pmatrix}, \ \vec{v} = \begin{pmatrix} A_{21} \\ A_{31} \\ \vdots \\ A_{N_c-1,1} \end{pmatrix}, \tag{1.6}$$

leading to the solution

$$p_i = a_i P \tag{1.7}$$

where we define $\vec{a} = \mathrm{M}^{-1}\vec{v}$. The flow rate Q becomes then

$$Q = \frac{1}{L}\sum_{i,j} q_{ij} = \frac{P}{L}\sum_{i,j} \sigma_{ij}(a_i - a_j); \tag{1.8}$$

comparing this result to Eq. 1.1 we can finally calculate the permeability of our model.

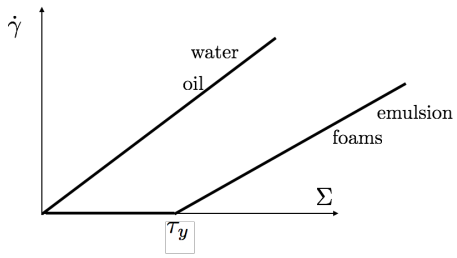

Figure 1.4: Shear rate $\dot{\gamma}$ as a function of the shear stress Σ for Newtonian fluids and Bingham plastics.

1.2 Rheology of non-Newtonian fluids: the Poiseuille law of a Bingham plastic

The Darcy's law does not capture the behavior of many fluids currently used for various applications. In hydraulic fracturing, for example, cracks induced by high-pressure fluid injection allow the flow of gas and oil [2]. The fracking fluids are emulsions of water and sand or other proppants needed to keep the paths open. Foams are used in the enhanced oil recovery (EOR) to avoid the viscous fingering instability [14]. Complex fluids are also employed for biomedical purposes. Different types of bone cements are employed in orthopaedics for the stabilization of osteoporotic compression fractures and the fixation of other weakening lesions such as tumours [3].
All the aforementioned applications involve yield stress fluids, namely liquids that are able to flow only above a finite yield stress, τ_y. In this work we will consider a particular kind of yield stress fluid called *Bingham plastic* [15]. In order to study the behaviour of a fluid, we can apply a shear stress to the fluid and measure its shear rate, namely the velocity of the shear deformation induced by the stress. While a Newtonian fluid flows and gives a shear rate for any finite value of shear stress, a Bingham plastic does not exhibit any shear rate (no flow and thus no velocity) until a certain stress τ_y is achieved, above which linearity is recovered (see Figure 1.4).

We now revisit the pore network model introduced in the previous Section for a Bingham plastic. The Poiseuille law for this type of fluid in the throat connecting the pores i and j should be modified in a non-linear way

$$q_{ij} = \begin{cases} \sigma_{ij}(\Delta p_{ij} - \tau_{ij}) \text{ if } \Delta p_{ij} > \tau_{ij} \\ 0 \qquad\quad \text{if } |\Delta p_{ij}| < \tau_{ij} \\ \sigma_{ij}(\Delta p_{ij} + \tau_{ij}) \text{ if } \Delta p_{ij} < -\tau_{ij} \end{cases} \tag{1.9}$$

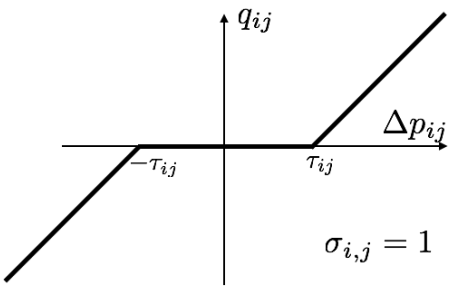

Figure 1.5: Plot of Equation 1.9, setting $\sigma_{ij} = 1$.

Comparing to Equation 1.2, the local pressure threshold τ_{ij} is introduced now, below which no flow occurs in the channel. In particular, for a cylindrical throat of length l and radius r_0, $\tau_{ij} = \tau_y l/r_0$. Note that while τ_y is constant as long as it's a characteristic of the fluid, the local thresholds τ_{ij} vary randomly as they depends on the throat geometry.

1.3 Bingham plastics in a porous lattice

Given the total pressure drop P and the configuration of random thresholds, the set of equations 1.9 together with Kirchhoff's conditions are closed, but very difficult to solve due to the non-linearity of the Poiseuille law for non-Newtonian fluids. Recent experiments [5] and numerical simulations [6] have shown that no flow is observed below a critical pressure drop P_0, and flow occurs only above it. In this regime, the flow curve is non linear with $Q \propto (P - P_0)^\beta$ and $\beta > 1$. At higher pressure, linearity is recovered and the flow invades homogeneously the material.
The separation from an arrested phase to a flowing one can be seen as a dynamical continuous phase transition, P being the control parameter and Q the order parameter. In this context, one expects to observe divergent correlation lengths and universality. Universal behaviour can be verified by changing the model in some small-scale detail (e.g. the structure of the network, or the distribution of the random thresholds), while the identification of divergent correlation lengths is much less understood. However, recent studies [7–9] tried to investigate the geometrical properties of the flowing regions and found that close to P_0 the flow is characterized by a phase separation [16] between flowing and non-flowing regions. We discuss now an algorithm that allows to determine the flow curve of a Bingham plastic and focus on the length of open channels close to P_0. The main result is that these lengths display a free-scale statistics giving a strong support to the existence of divergent correlation lengths.

The numerical method discussed here applies to any lattice type [17], but we consider for simplicity the 2-dimensional square lattice of Figure 1.6. The fluid flows from inlet to the outlet node, whose pressures are set respectively to P and 0. The crucial observation is that, for a given pressure difference P, the flow occurs only in a set of open throats, $\mathcal{L}(P)$. Once $\mathcal{L}(P)$ is known, the solution of the local pressure for every node can be found performing a linear calculation analogous to the one shown in Section 1.1 for Newtonian fluids. Recalling the definition 1.3 of the matrix A and defining also the anti-symmetric matrix I that contains the information on the directions of the flow trough all the throats (ij)

$$I_{ij} = \begin{cases} \sigma_{ij} \text{ if } (ij) \in \mathcal{L}(P) \text{ and the flow is in direction } i \text{ to } j \\ -\sigma_{ij} \text{ if } (ij) \in \mathcal{L}(P) \text{ and the flow is in direction } j \text{ to } i \\ 0 \quad \text{if } (ij) \notin \mathcal{L}(P) \end{cases} \tag{1.10}$$

the Kirchhoff condition combined with Eq. 1.9 writes now

$$\sum_{j=i}^{N_c} A_{ij}(p_i - p_j) = \sum_{j=i}^{N_c} I_{ij}\tau_{ij}. \tag{1.11}$$

Rewriting this in the matrix form

$$\mathrm{M}\vec{p} = \vec{u} + P\vec{v}, \tag{1.12}$$

where M, $\vec{p}$ and $\vec{v}$ are the same of 1.6, while

$$\vec{u} = \begin{pmatrix} \sum_{j=i}^{N_c} I_{2j}\tau_{2j} \\ \sum_{j=i}^{N_c} I_{3j}\tau_{3j} \\ \vdots \\ \sum_{j=i}^{N_c} I_{N_c-1,j}\tau_{N_c-1,j} \end{pmatrix}, \tag{1.13}$$

the solution for p_i becomes

$$p_i = a_i P + b_i \tag{1.14}$$

where $\vec{a} = \mathrm{M}^{-1}\vec{v}$ and $\vec{b} = \mathrm{M}^{-1}\vec{u}$. So, for a given P, the solution for the local pressure p_i of the i-th node is still linear as in the Newtonian case, and its coefficients depend on $\mathcal{L}(P)$.

In order to determine the set of open throats $\mathcal{L}(P)$, we follow an iterative procedure, starting from the minimal pressure P_0 needed to open the first channel connecting the inlet and the outlet pores, that is obtained by finding, among all the paths connecting

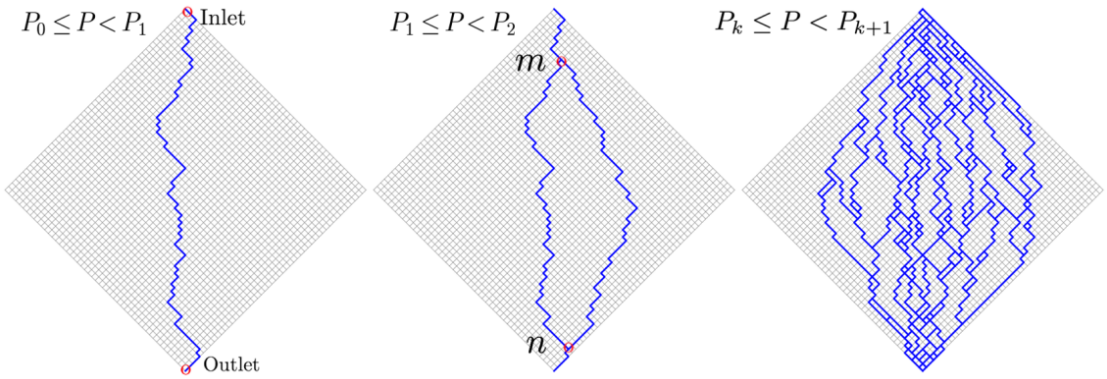

Figure 1.6: The flowing path network at different applied pressures for a system of size $L = 100$.

the inlet and outlet nodes, the one that minimize the sum of the thresholds crossed by it:

$$P_0 = \min_{C \in \mathcal{C}_{in-out}} \sum_{(ij) \in C} \tau_{ij} \tag{1.15}$$

where we call $\mathcal{C}_{in-out}$ the set of paths from the inlet to the outlet node.

- If $P < P_0$ all the channels of the network are closed, so $\mathcal{L}(P) = \emptyset$ and no fluid is flowing in the medium.
- At $P = P_0$ a first channel, corresponding to the path that realizes the minimum, is opened and the fluid starts to flow in it; calling this channel C_0 we have $\mathcal{L}(P_0) = C_0$.
- For slightly larger values of pressure the flow remains restricted to this channel and thus $\mathcal{L}(P \gtrsim P_0) = \mathcal{L}(P_0)$.
- Increasing even more the pressure, at a certain point the pressure needed to open a second channel, namely P_1, is reached; so $\mathcal{L}(P_1) = C_0 + C_1$ where C_1 is the new channel opened at $P = P_1$.
- The procedure is repeated iteratively: if P_k is the pressure needed to open the $(k+1)$-th channel, we have $\mathcal{L}(P_k) = \mathcal{L}(P_{k-1}) + C_k$ where C_k is the new channel.

Summarizing, for a given realization of the thresholds τ_{ij}, the enlargements of $\mathcal{L}(P)$ occur at precise pressure values $P_0 < P_1 < P_2 < \cdots < P_k < \ldots$, as shown in Fig. 1.6. For every change of $\mathcal{L}(P)$, the coefficients a_i and b_i of the solution for p_i (Eq. 1.14) are modified, giving the non-linearity of the problem. When all channels are open, for higher pressure $\mathcal{L}(P)$ will remain the same and linearity is recovered (see the left plot of Figure 1.7). In principle, the channel can be non-directed, i.e. can involve throats

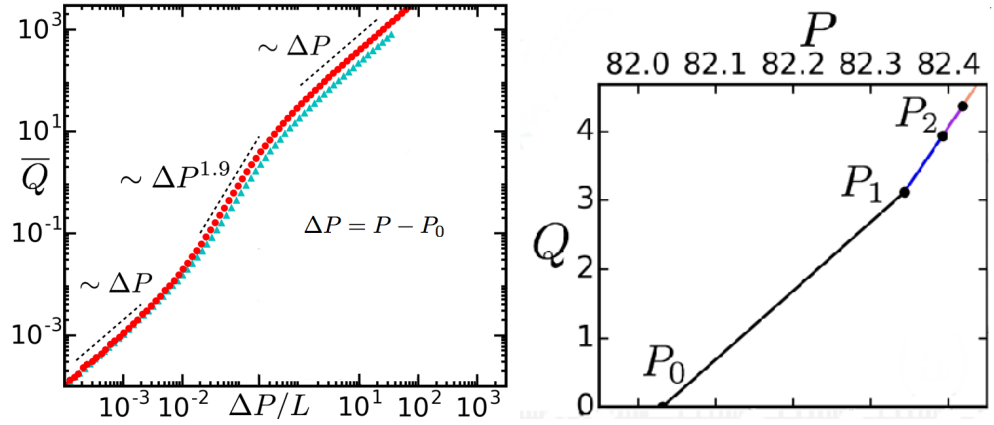

Figure 1.7: (Numerical results presented in [17]) Left: The mean flow curve $\overline{Q}$ for a given $\Delta P = P - P_0$ averaged over more than 200 realizations. The thresholds are uniformly distributed in the interval $[2 - \sqrt{3}/5, 2 + \sqrt{3}/5]$. Circles and triangles correspond to $L = 64$ and $L = 128$ respectively. Right: The flow curve of a single realization for $P \gtrsim P_0$ ($L = 50$).

where the flow goes away from the outlet node (goes upward in the lattice of Figure 1.7), but in practice the statistics is dominated by the directed ones [7, 18] so we restrict our analysis to them.

To find P_k, and the corresponding $\mathcal{L}(P_k)$, knowing $\mathcal{L}(P_{k-1})$, we should consider the set A_{k-1} of all pairs of active nodes belonging to $\mathcal{L}(P_{k-1})$. For each node pair $(m, n) \in A_{k-1}$, we consider the set $C_{m,n}$ of all paths that connect n and m and that avoid any other intersection with $\mathcal{L}(P_{k-1})$ beyond the end points. The optimal path among $C_{m,n}$ has a threshold

$$E_{mn} = \min_{C \in \mathcal{C}_{mn}} \sum_{(ij) \in C} \tau_{ij} \tag{1.16}$$

For a given $P > P_{k-1}$, if, for all pairs of nodes $(n, m) \in A_{k-1}$, the threshold E_{mn} is larger than the corresponding pressure difference $\Delta p_{mn}(P)$, then no new channels appear and $\mathcal{L}(P_k) = \mathcal{L}(P_{k-1})$. Expressing p_m and p_n in terms of a_m , b_m and a_n , b_n respectively, the pressure P_k is then determined by

$$P_k = \min_{(m,n) \in A_{k-1}} \frac{E_{mn} - (b_m - b_n)}{a_m - a_n}; \tag{1.17}$$

In particular, we can provide a deeper understanding on how the non-linearity of the flow is approached from small values of $P - P_0$. In the right plot of Figure 1.7, we present the flow curve for a single realization for $P \gtrsim P_0$; we can see that the exact linearity terminates at $P = P_1$, when a second path opens and the permeability of the system

changes; for $P_1 \leq P < P_2$, Q is still linear but with a different slope. Simplifying Eq. 1.17, P_1 is calculated as follows

$$P_1 = P_0 + L \min_{(m,n)\in\mathcal{L}(P_0)} \left(\frac{\delta E_{mn}}{\ell_{mn}} \right); \tag{1.18}$$

here ℓ_{mn} is the distance along the flow direction between the nodes m and n, and $\delta E_{mn} = E_{mn} - E^0_{mn}$, with E^0_{mn} the sum of the thresholds along C_0 between n and m, while E_{mn} is given by Eq. 1.16, where the paths included in $\mathcal{C}_{mn}$ avoid any intersection with C_0, apart from the ones in m and n. The minimizations provided in Equations 1.15 and 1.18 are performed using the Dijkstra optimization algorithm; a variant of this algorithm, developed and used in this thesis work, will be discussed in Section 3.2.2.

1.4 Mapping with directed polymers in random media

As already mentioned it is tempting to interpret the onset of the flow at P_0 as a dynamical phase transition and expect scale-free behaviour close to P_0. This is actually observed numerically in the statistics of the length of the second channel, i.e. the channel that opens at P_1. As shown in Figure 1.8 we observe that the probability distribution π_ℓ of the length $\ell = \ell_{mn}$ of this channel is a power law decaying as

$$\pi_\ell \propto \frac{1}{\ell}\,. \tag{1.19}$$

Note that the mean length of the second channel $\overline{\ell}$ (here the overline has the meaning of an average over all realizations of the disorder) diverges, and its divergence can be interpreted as the divergence of the correlation length at the critical point. This observation has been performed only for the 2-dimensional square lattice, but should be confirmed in higher dimension. In this thesis we study in detail the case of the 3-dimensional lattice, and we will show that that divergence is even stronger. To make progress on the statistics of ℓ, we use the mapping between this problem and the one of directed polymers in random media. The search of the first channel in a 2-dimensional lattice via the minimization expressed in Equation 1.15 is equivalent to find the ground state of a $(1+1)$-dimensional directed polymer on a lattice in a random medium, and P_0 corresponds to its energy. The second channel, whose minimization is provided by Equation 1.18, can be instead seen as a first excited state of the polymer, and δE_{mn} corresponds to the difference between its energy and the ground state one. Note that the two polymers coincide except along the segment between the nodes m and n, where the avoid

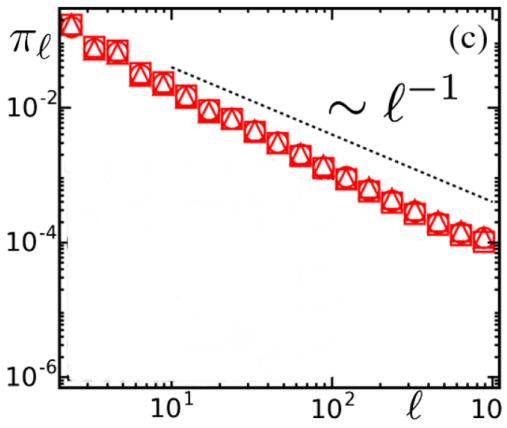

Figure 1.8: (Numerical results presented in [17]) The PDF of lengths of the second open paths π_ℓ. Circles, squares and triangles correspond to different threshold distributions: uniform, Gaussian and exponential, respectively

each other. This mapping from $(1+1)$-dimensional directed polymer to the Bingham flow on a 2-dimensional lattice could be generalized to any lattice and any dimension. The fact that we have considered only directed channel for the flow in the lattice, as we mentioned before, is actually crucial to the mapping. In the following Section, we show the connection between π_ℓ and the statistical properties of the first excitation on the ground state of a directed polymer in random media.

1.4.1 Relation between the second channel's length and the energy gap statistics

We now show that the behaviour of π_ℓ is the same of $\rho_\ell(\delta E_{mn} \to 0)$, namely the probability distribution of the energy gap for $\delta E_{mn} \to 0$ [17]. In particular, supposing that $\rho_\ell(\delta E_{mn} \to 0)$ scales as a power law of ℓ

$$\rho_{\ell_{mn}}(\delta E_{mn} \to 0) \sim \frac{1}{\ell^\alpha}, \tag{1.20}$$

we show that equally

$$\pi_\ell \sim \frac{1}{\ell^\alpha}. \tag{1.21}$$

Consider all pairs of node (m,n) along the ground state with a given distance along the directed axis $l_{mn} = l$; these can be generally written as $(m, m+\ell)$ with $m = 1, \ldots, L-\ell$.

Now we select the minimal energetic excitation among them

$$\delta e_\ell = \min_{\ell_{mn}=\ell} \delta E_{mn} = \min_{\ell_{m,m+\ell}} \delta E_{mn}. \tag{1.22}$$

δe_ℓ is the minimum among $L-\ell$ random variables that are identically distributed but not independent, displaying indeed strong correlations between close couple [e.g. $(m, m+\ell)$ and $(m+1, m+\ell+1)$] as their correspondent channels present large overlaps. It is reasonable then to assume that the effective number of independent variables scales as the number of non-overlapping blocks $N_\ell = L/\ell$ and the statistics of δe_ℓ is given by the minimum among them. This means that the probability that δe_ℓ is higher than a certain value x corresponds to the probability that all the N_ℓ independent variables are higher than x:

$$\begin{aligned} \text{Prob}[\delta e_\ell > x] &= \left(1 - \int_0^x d(\delta E)\rho_\ell(\delta E)\right)^{N_\ell} \\ &\simeq \exp\left(-N_\ell \int_0^x d(\delta E)\rho_\ell(\delta E)\right) \\ &\simeq \exp\left(-N_\ell \rho_\ell(0) x\right) \\ &\simeq \exp\left(-\frac{N_\ell}{\ell^\alpha} x\right) \end{aligned} \tag{1.23}$$

where in the first passage we consider the limit for large N_ℓ, while the approximation in the last passage is performed using Eq. 1.20. In order to get ΔP_1, we have to find the minimum energy cost per length among all the possible lengths $\ell = 2, 3, \dots L$

$$\frac{\Delta P_1}{L} = \min_\ell \frac{\delta e_\ell}{\ell} \tag{1.24}$$

Hence, using Equation 1.23 we obtain the distribution of the gap $\Delta P_1/L$.

$$\begin{aligned} \text{Prob}[\frac{\Delta P_1}{L} > x] &= \prod_{\ell=2}^{L} \text{Prob}\left[\frac{\delta e_\ell}{\ell} > x\right] \\ &\simeq \prod_{\ell=2}^{L} \exp\left(-\frac{N_\ell}{\ell^{\alpha-1}} x\right) \\ &= \exp\left(-\left(\sum_{\ell=2}^{L} \frac{N_\ell}{\ell^{\alpha-1}}\right) x\right), \end{aligned} \tag{1.25}$$

If we introduce now the variable $\omega_\ell = \delta e_\ell/\ell$, taking the derivative of Equation 1.23 we obtain the PDF of ω_ℓ

$$p_\ell(\omega_\ell) \simeq \frac{N_\ell}{\ell^{\alpha-1}} e^{-\frac{N_\ell}{\ell^{\alpha-1}}\omega_\ell}. \tag{1.26}$$

Finally, the statistics of the size of the second path π_ℓ is obtained considering that $\omega_{\ell'} > \omega_\ell \; \forall \; \ell' \neq \ell$:

$$\begin{aligned}
\pi_\ell &= \int_0^{+\infty} d\omega_\ell \, p_\ell(\omega_\ell) \prod_{\ell' \neq \ell} \int_{\omega_\ell}^{+\infty} d\omega_{\ell'} \, p_{\ell'}(\omega_{\ell'}) \\
&= \int_0^{+\infty} d\omega_\ell \, \frac{N_\ell}{\ell^{\alpha-1}} e^{-\frac{N_\ell}{\ell^{\alpha-1}}\omega_\ell} \prod_{\ell' \neq \ell} \int_{\omega_\ell}^{+\infty} d\omega_{\ell'} \, \frac{N_{\ell'}}{\ell'^{\alpha-1}} e^{-\frac{N_{\ell'}}{\ell'^{\alpha-1}}\omega_{\ell'}} \\
&= \int_0^{+\infty} d\omega_\ell \, \frac{N_\ell}{\ell^{\alpha-1}} e^{-\frac{N_\ell}{\ell^{\alpha-1}}\omega_\ell} \prod_{\ell' \neq \ell} e^{-\frac{N_{\ell'}}{\ell'^{\alpha-1}}\omega_\ell} \\
&= \int_0^{+\infty} d\omega_\ell \, \frac{N_\ell}{\ell^{\alpha-1}} e^{-\left(\sum_{\ell'} \frac{N_{\ell'}}{\ell'^{\alpha-1}}\right)\omega_\ell} \\
&= \left(\sum_{\ell'} \frac{N_{\ell'}}{\ell'^{\alpha-1}} \right)^{-1} \frac{N_\ell}{\ell^{\alpha-1}} \sim \ell^{-\alpha}.
\end{aligned} \tag{1.27}$$

The behaviour of π_ℓ is then the same of $\rho_{\ell_{mn}}(\delta E_{mn} \to 0)$ and this was confirmed numerically for the 2-dimensional square lattice:

$$\rho_{\ell_{mn}}(\delta E_{mn} \to 0) \sim \pi_\ell \sim \frac{1}{\ell}, \tag{1.28}$$

setting the value of α equal to one.

1.4.2 Relation between the small energy gap statistics and the non-crossing probability

Consider directed polymers in random media that grow from a certain point at time 0 and ends at the same point at time t, and we impose that the polymers do not cross with the exception of the starting and the ending points. We are interested in the probability $\rho_t(\Delta E \to 0)$ that, for a fixed t, the energy gap ΔE between the ground state and the first excited state tends to zero. When this occurs, the ground state is two-fold degenerate, meaning that the first excited polymer acts like a second independent ground state. A different way to verify whether the ground state is two-fold degenerate is to construct the ground state of two polymers that start and end in two distinct, but close to each

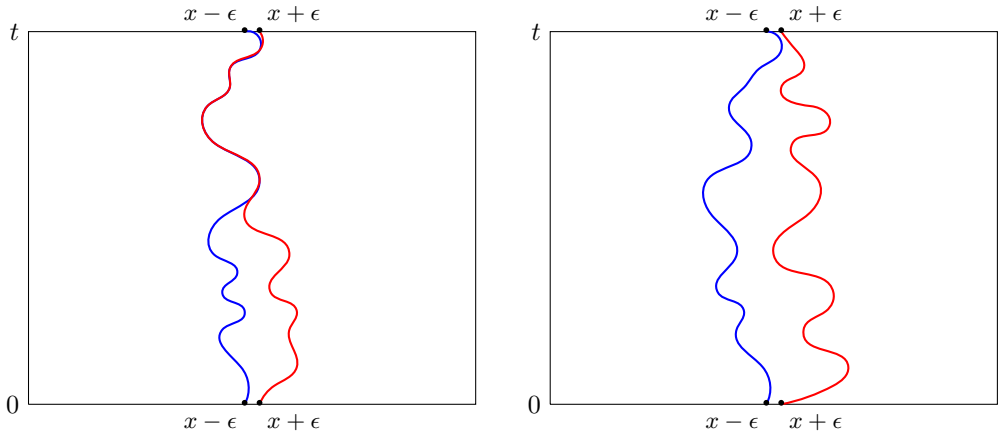

Figure 1.9: Draw of two ground state polymers that starts and ends at two distinct points separated by 2ϵ. Left: the two polymers present a finite overlap. Right: the two polymers have no overlap.

other, points (see Figure 1.9). Two possibilities should be considered

1. The ground states have a finite overlap; in this case the ground state is unique and the first non-intersecting excited state has an higher energy.

2. The two ground states have no overlap and the energy gap of the first non-intersecting excited state is zero meaning that we have double degenerate ground state.

The non-crossing probability $p(t)$, namely the probability that the two ground state polymers never cross from 0 to t, is then naturally identified with $\rho_t(\Delta E \to 0)$, and thus with π_l. In this thesis we study how $p(t)$ scales with t both in absence and in presence of disorder. Our results of $p(t)$ allow us to infer the behaviour of $\rho_t(\Delta E \to 0)$ and thus of π_ℓ for large ℓ.

1.5 Summary of the results

In this thesis we focused on the calculation of the non crossing probability $p(t)$ for two different stochastic processes in $(1+1)$ and $(2+1)$ dimensions.
The first results are for free directed polymers, namely each polymer configuration is a Brownian trajectory and the Brownian time coincide with the directed direction. This problem has been studied in Chapter 2 using first passage techniques (method of images, exact relation from Feller and Redner . . .). In dimension $(1+1)$ we found a simple power

law decay, valid in the thermodynamic limit $t \to +\infty$:

$$p(t) \sim \frac{1}{t}; \tag{1.29}$$

in dimension $(2+1)$ the decay is instead much slower

$$p(t) \sim \frac{1}{\log^2(t)}, \tag{1.30}$$

and above this dimension we expect that the two polymers never cross with a finite probability (this is a consequence of the celebrated Pólya's theorem [19]). At the end of Chapter 2 we show that for $(1+1)$ dimension the free result is recovered, in average, also for the second class of stochastic processes we considered, namely the directed polymers in random media:

$$\overline{p_\eta(t)} = p(t) \sim \frac{1}{t}. \tag{1.31}$$

As a consequence, the first channel that open above P_0 are scale free and their distribution $\pi_\ell \sim 1/\ell$ in 2 dimension.

In Chapter 3 we turn to numerical simulations on discrete lattice, both for free directed polymers as well as the ground states of directed polymers in random media. In the disordered case the ground state are efficiently determined by a variant of the Dijkstra algorithm. We confirmed the analytical results for the free case and the $(1+1)$ disordered case. In $(2+1)$ dimensions we found that $\overline{p_\eta(t)}$ displays a crossover in time: at short time it seems to match the correspondent free case, but at longer time it decays faster as

$$\overline{p_\eta(t)} \sim \frac{1}{t^\alpha} \text{ with } 0.5 \lesssim \alpha \lesssim 0.75 \tag{1.32}$$

Even if the asymptotic behaviour is not precise we can conclude that for a 3-dimensional system the non-Newtonian channel above P_0 are longer then in the 2-dimensional one as, for sure, $\alpha < 1$. This implies that the mean length is still divergent, as we expect at the critical point of a phase transition.

Chapter 2

Directed Polymers

2.1 General definition

We can consider a polymer configuration as a trajectory of a particle moving between two points. In this Chapter we discuss about polymers in the continuum limit, meaning that the trajectories occur in a continuous space. A polymer is called *directed* if the particle always moves from the initial towards the final point along a trajectory that does not contain loops or overhangs. Formally, this means that the configuration of the directed polymer in $d+1$ dimensions can be parametrized by giving d transverse coordinates $\vec{x} = (x_1, \ldots, x_d) \in \mathbb{R}$ as a function of the longitudinal coordinate $\tau \in \mathbb{R}$, which gives the distance along the path and can be regarded as a "time" axis (see Figure 2.1).

Here two classes of directed polymers are studied: *free directed polymers* and *directed polymers in disordered media* [20–24].

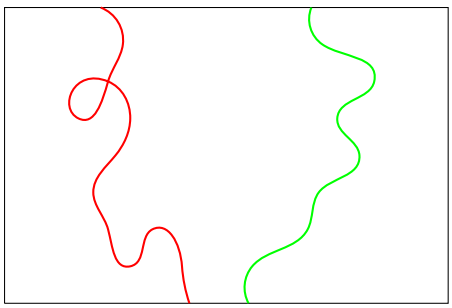

Figure 2.1: Draw of two polymers in 2 dimensions, one of which isn't directed (in red), while the other is (in green).

- **Free directed polymers.** The particle is not subjected to any external force and is free to move in the space. If we consider a free directed polymer $\vec{x}(t)$ that starts and ends at time 0 and t respectively, we can then define its energy $E[\vec{x}(t)]$ as a functional of $\vec{x}(t)$

$$E[\vec{x}(t)] = \int_0^t d\tau \, \frac{1}{4D} \left(\frac{d\vec{x}}{d\tau} \right)^2 ; \tag{2.1}$$

$\frac{1}{4D} \left(\frac{\mathrm{d}\vec{x}}{\mathrm{d}\tau} \right)^2$ is the elastic energy term, which is minimized for straight paths, and D characterizes the stiffness of the polymer.
The partition function $Z(\vec{x}; \vec{y}|t)$ of a free directed polymer that starts at time 0 from the point $\vec{x}(0) = \vec{x}$ and ends after a time t at $\vec{x}(t) = \vec{y}$, at a fixed finite temperature T, is thus the functional integral of the Boltzmann weight $e^{-\beta E[\vec{x}(t)]}$, where $\beta = 1/T$ (we set Boltzmann's constant $k_B = 1$ so that the temperature is measured in energy units), over all the paths $\vec{x}(t)$ that start from $\vec{x}$ and end at $\vec{y}$:

$$Z(\vec{x}; \vec{y}|t) := \int_{\vec{x}(0)=\vec{x}}^{\vec{x}(t)=\vec{y}} \mathrm{D}[\vec{x}] \, e^{-\beta E[\vec{x}(t)]} = \int_{\vec{x}(0)=\vec{x}}^{\vec{x}(t)=\vec{y}} \mathrm{D}[\vec{x}] \, e^{-\int_0^t d\tau \, \frac{1}{4D} \left(\frac{d\vec{x}}{d\tau} \right)^2} ; \tag{2.2}$$

in the last passage we set an unitary temperature. This integral is solvable, and $Z(\vec{x}; \vec{y}|t)$ turns out to have the same form of the Brownian propagator G_D with diffusion constant D:

$$Z(\vec{x}; \vec{y}|t) = G_D(\vec{x} - \vec{y}, t) = \frac{e^{-\frac{(\vec{x}-\vec{y})^2}{4Dt}}}{(4\pi D t)^{\frac{d}{2}}}. \tag{2.3}$$

- **Directed polymers in disordered media.** In this case each point of the $(d+1)$-dimensional space $(\vec{x}, \tau)$ is associated with a local potential $\eta(\vec{x}, \tau)$. We model a *disordered* (or *random*) medium by taking η to be uncorrelated noise, for which:

$$\overline{\eta(\vec{x}_1, t_1)\eta(\vec{x}_2, t_2)} = 2c \, \delta^{(d)}(\vec{x}_1 - \vec{x}_2)\delta(t_1 - t_2). \tag{2.4}$$

where the overline denotes averages over all the realization of η, while c gives the strength of the random potential. The energy $E_\eta[\vec{x}(t)]$ related to a directed polymer $\vec{x}(t)$ in a given realization of the potential η is now

$$E_\eta[\vec{x}(t)] = \int_0^t d\tau \, \left[\frac{1}{4D} \left(\frac{d\vec{x}}{d\tau} \right)^2 + \eta(\vec{x}(\tau), \tau) \right] ; \tag{2.5}$$

$\eta(\vec{x}, t)$ could be thought as the energy it costs the polymer to pass through the site

$(\vec{x}, t)$, so E_η is minimized for paths picking out the minimal energy sites.
The partition function Z_η of a directed polymer in a given realization of the potential η is then

$$Z_\eta(\vec{x}; \vec{y}|t) = \int_{\vec{x}(0)=\vec{x}}^{\vec{x}(t)=\vec{y}} \mathrm{D}[\vec{x}]\, e^{-\int_0^t d\tau \left[\frac{1}{4D}\left(\frac{d\vec{x}}{d\tau}\right)^2 + \eta(\vec{x}(\tau),\tau)\right]}. \tag{2.6}$$

Note that we can consider free directed polymers as a subcase of the disordered ones, if we set $\eta(\vec{x}, t) \equiv 0\ \forall \vec{x}, t$.

Now let's consider n directed polymers starting respectively from n fixed positions $\vec{x}_{A_1}$, $\vec{x}_{A_2}$, ..., $\vec{x}_{A_n}$ and, after a time t, ending at $\vec{y}_{A_1}$, $\vec{y}_{A_2}$, ..., $\vec{y}_{A_n}$; supposing they don't interact each other, in general the partition function of these polymers is simply the product of the partition functions of these single polymers

$$Z_\eta(\vec{x}_{A_1}, \vec{x}_{A_2}, ..., \vec{x}_{A_n}; \vec{y}_{A_1}, \vec{y}_{A_2}, ..., \vec{y}_{A_n}|t) = \prod_{i=1}^{n} Z_\eta(\vec{x}_{A_i}; \vec{y}_{A_i}|t) \tag{2.7}$$

In particular for two polymers, that we can label 'A' and 'B',

$$Z_\eta(\vec{x}_A, \vec{x}_B; \vec{y}_A, \vec{y}_B|t) = Z_\eta(\vec{x}_A; \vec{y}_A|t) Z_\eta(\vec{x}_B; \vec{y}_B|t). \tag{2.8}$$

The properties 2.7 and 2.8 are valid also for polymers in a discrete space that moves on a lattice; however, we will discuss about polymers in the discrete limit in the next Chapter.

2.2 Non-crossing probability: general formula

Let's consider then the case of two directed polymers in a disordered medium that both start and end at time 0 and t respectively. We are now interested in finding the *non-crossing probability*, namely the probability that these two polymers never intersect during the time interval $]0, t[$, i.e. they are never situated in the same point at any time $0 < \tau < t$.
In $d = 1$ dimension, in a given realization η of the potential, this probability could be expressed in terms of partition functions of single polymers

$$p_\eta(x_A, x_B; y_A, y_B|t) = 1 - \frac{Z_\eta(x_B; y_A|t) Z_\eta(x_A; y_B|t)}{Z_\eta(x_A; y_A|t) Z_\eta(x_B; y_B|t)}. \tag{2.9}$$

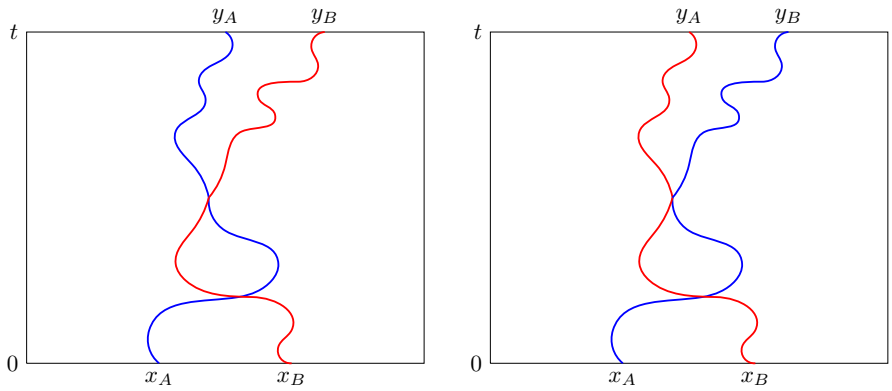

Figure 2.2: Left: Two directed polymers in $d = 1$ (one going from x_A to y_A, the other from x_B to y_B) intersecting at least once. Right: Two directed polymer with the same statistical weight but exchanged ends.

according to 2.8, $Z_\eta(x_B; y_A|t)Z_\eta(x_A; y_B|t)$ is the partition function of two generic polymers that start from x_A, x_B and end at y_A, y_B respectively; $Z_\eta(x_A; y_A|t)Z_\eta(x_B; y_B|t)$ includes instead all paths of the same kind but with y_A, y_B exchanged, since all paths with at least one intersection can be obtained from paths with y_A, y_B exchanged [25,27]. Their ratio gives then the probability that the two polymers crosses at least once. In the Appendix A.1 we report a proof for 2.9 based on the method of images.

If we consider the situation in which for both polymers the initial and final points are the same, i.e. $x_A = y_A$ and $x_B = y_B$ and if we set $\eta \equiv 0$ (free case), using Eq. 2.3 we have

$$Z_{\eta\equiv 0}(x; y|t) = G_D(x - y, t) = \frac{e^{-\frac{(x-y)^2}{4Dt}}}{\sqrt{4D\pi t}} \tag{2.10}$$

so the probability 2.9 becomes

$$p(\Delta x, t) := p_{\eta\equiv 0}(x_A, x_B; x_A, x_B|t) = 1 - e^{-\frac{\Delta x^2}{2Dt}} \xrightarrow[t>>\Delta x]{} \frac{\Delta x^2}{2Dt}, \tag{2.11}$$

where $\Delta x := x_B - x_A$; in the last passage it is shown that, for times much larger than Δx, the probability goes to 0 as $1/t$.
Since, as explained in the Appendix, for $d \geq 2$ the method of images is not valid anymore, we have to look for an alternative expression for the non-crossing probability. We observe that the probability that two polymers cross at least once could be generally written as the ratio between the partition function of two DP that cross at least once and the partition function of two generic directed polymers, that may cross or not; in this way

we can write

$$\begin{aligned} p_\eta(x_A, x_B; y_A, y_B|t) &= 1 - \frac{\text{partition function of two crossing polymers}}{Z_\eta(x_A; y_A|t) Z_\eta(x_B; y_B|t)} \\ &= 1 - \frac{\int_0^t d\tau \int_{\mathbb{R}^d} d\vec{z}\, \tilde{Z}(\vec{x}_A, \vec{x}_B; \vec{z}, \vec{z}|\tau) Z(\vec{z}, \vec{z}; \vec{y}_A, \vec{y}_B|t-\tau)}{Z(\vec{x}_A; \vec{y}_A|t) Z_(\vec{x}_B; \vec{y}_B|t)}; \end{aligned} \tag{2.12}$$

Looking at the numerator of the last member of 2.12, we call $\tilde{Z}(\vec{x}_A, \vec{x}_B; \vec{z}, \vec{z}|\tau)$ the partition function of a pair of directed polymers that *never* intersect before τ, when they cross reaching both $\vec{z}$; $Z(\vec{z}, \vec{z}; \vec{y}_A, \vec{y}_B|t-\tau)$ is instead the normal partition function of two DP that starts both from $\vec{z}$ at time τ, meaning that they could possibly cross other times before reaching respectively $\vec{y}_A$ and $\vec{y}_B$ at time t. In order to count all pairs of paths of this kind, we have to integrate over all points $\vec{z}$ in the d-dimensional space and over all time τ in the interval $]0, t[$. Note that this general formula should be valid for any d.
While Eq. 2.6 gives an expression for Z_η, $\tilde{Z}_\eta$ is unknown; however, it is possible to perform calculations for the case of free directed polymers, as shown in the following Section.

2.3 Explicit results for the free case

The partition function of two directed polymers that, starting from $\vec{x}_A$ and $\vec{x}_B$ respectively, ends both at $\vec{z}$, could be thus written as the product of two free propagators with the same diffusion constant

$$Z(\vec{x}_A; \vec{y}_A|t) Z_(\vec{x}_B; \vec{y}_B|t) = G_D(\vec{x}_A - \vec{z}, \tau) G_D(\vec{x}_B - \vec{z}, \tau). \tag{2.13}$$

It is useful to introduce the coordinate of the center of mass and of the relative distance of the polymers

$$\vec{x}_{CM} = \frac{\vec{x}_A + \vec{x}_B}{2}, \quad \Delta\vec{x} = \vec{x}_B - \vec{x}_A; \tag{2.14}$$

it's easy to show that, rewriting Eq. 2.13 in the new coordinates, we still obtain a product of two free propagators, but both with a different value of the diffusion constant

$$\begin{aligned} G_D(\vec{x}_A-\vec{z},\tau)G_D(\vec{x}_B-\vec{z},\tau) &= \frac{e^{-\frac{(x_A-z)^2}{4Dt}}}{(4\pi Dt)^{\frac{d}{2}}}\frac{e^{-\frac{(x_B-z)^2}{4Dt}}}{(4\pi Dt)^{\frac{d}{2}}} \\ &= \frac{1}{(4\pi Dt)^d}e^{-\frac{\frac{\vec{x}_A^2}{2}+\frac{\vec{x}_B^2}{2}+\vec{x}_A\vec{x}_B+\vec{z}^2-2(\vec{x}_A+\vec{x}_B)\vec{z}+2\vec{z}^2+\frac{\vec{x}_A^2}{2}+\frac{\vec{x}_B^2}{2}-\vec{x}_A\vec{x}_B}{4Dt}} \\ &= \frac{e^{-\frac{\left(\frac{\vec{x}_A+\vec{x}_B}{2}-\vec{z}\right)^2}{2Dt}}}{(2\pi Dt)^{\frac{d}{2}}}\frac{e^{-\frac{(\vec{x}_B-\vec{x}_A)^2}{8Dt}}}{(8\pi Dt)^{\frac{d}{2}}} \\ &= G_{\frac{D}{2}}(\vec{x}_{CM}-\vec{z},\tau)G_{2D}(\Delta\vec{x},\tau); \end{aligned} \tag{2.15}$$

Observe that, if we impose that these two DP never cross before meeting in $\vec{z}$, we are asking that the difference of their coordinates never go to $\vec{0}$ before τ, while the average position has no restrictions. We can then write

$$\tilde{Z}(\vec{x}_A,\vec{x}_B;\vec{z},\vec{z}|\tau) = G_{\frac{D}{2}}(\vec{x}_{CM}-\vec{z},\tau)F_{2D}(\Delta\vec{x},\tau); \tag{2.16}$$

where $F_{2D}(\Delta\vec{x},\tau)$ is the partition function of a free DP that diffuses with a diffusion constant of $2D$, but never goes to $\vec{0}$ before t. In this way, the numerator of the ratio on the right side of Eq. 2.12 can be written as

$$\begin{aligned} &\int_0^t d\tau\int_{\mathbb{R}^d}d\vec{z}\,\tilde{Z}(\vec{x}_A,\vec{x}_B;\vec{z},\vec{z}|\tau)Z(\vec{z},\vec{z};\vec{x}_A,\vec{x}_B|t-\tau) = \\ &= \int_0^t d\tau\int_{\mathbb{R}^d}d\vec{z}\,G_{\frac{D}{2}}(\vec{x}_{CM}-\vec{z},\tau)F_{2D}(\Delta\vec{x},\tau)G_D(\vec{z}-\vec{y}_A,t-\tau)G_D(\vec{z}-\vec{y}_B,t-\tau); \end{aligned} \tag{2.17}$$

Let's consider for simplicity the case for which $\vec{x}_A=\vec{y}_A$ and $\vec{x}_B=\vec{y}_B$. The integral in $d\vec{z}$ gives then a rather simple solution valid for all d

$$\int_{\mathbb{R}^d}d\vec{z}\,G_{\frac{D}{2}}(\vec{x}_{CM}-\vec{z}.\tau)G_D(\vec{z}-\vec{x}_A,t-\tau)G_D(\vec{z}-\vec{x}_B,t-\tau) = (2D\pi t)^{-\frac{d}{2}}G_{2D}(\Delta\vec{x},t-\tau), \tag{2.18}$$

and since $G_D(0,t)=(4D\pi t)^{-\frac{d}{2}}$, Eq. 2.12 becomes

$$p(\vec{x}_A,\vec{x}_B,t) = 2^{\frac{3d}{2}}(D\pi t)^{\frac{d}{2}}\int_0^t \mathrm{d}\tau\, F_{2D}(\Delta\vec{x},\tau)G_{2D}(\Delta\vec{x},t-\tau) = 2^{\frac{3d}{2}}(D\pi t)^{\frac{d}{2}}I(\Delta\vec{x},t). \tag{2.19}$$

where we have defined

$$I(\Delta\vec{x},t) := \int_0^t d\tau\, F_{2D}(\Delta\vec{x},\tau)G_{2D}(\Delta\vec{x},t-\tau). \tag{2.20}$$

In order to solve this integral, consisting in a convolution between F_{2D} and G_{2D}, it is convenient to perform a Laplace transform of it[1]; using the fact that the Laplace transform of a convolution of two functions is the product of the Laplace transform of the two functions; in this way the expression is easier to manage, and after some passages we can do the inverse Laplace transform in order to obtain an analytical solution for 2.20. Indicating with $\hat{I}(\Delta\vec{x},s)$ the Laplace transform of Eq. 2.20

$$\hat{I}(\Delta\vec{x},s) = \int_0^{+\infty} dt \int_0^t d\tau\, F_{2D}(\Delta\vec{x},\tau)G_{2D}(\Delta\vec{x},t-\tau)e^{-st} = \hat{F}_{2D}(\Delta\vec{x},s)\hat{G}_{2D}(\Delta\vec{x},s); \tag{2.23}$$

where $\hat{F}_{2D}$ and $\hat{G}_{2D}$ are the Laplace transform of F_{2D} and G_{2D} respectively. An expression of F_{2D} as a function of G_{2D} has been derived in the Appendix A.2, following the method developed by Feller [28]:

$$\hat{F}_{2D}(\Delta\vec{x},s) = \frac{\hat{G}_{2D}(\Delta\vec{x},s)}{\hat{G}_{2D}(\vec{0},s)}; \tag{2.24}$$

in this way we directly get

$$\hat{I}(\Delta\vec{x},s) = \frac{\hat{G}^2_{2D}(\Delta\vec{x},s)}{\hat{G}_{2D}(\vec{0},s)}; \tag{2.25}$$

In generic dimension d the Laplace transform of the free propagator $G_D(\Delta\vec{x},t)$ is

$$\hat{G}_D(\Delta\vec{x},s) = \int_0^{+\infty} dt\, \frac{e^{-\frac{\Delta x^2}{4Dt}}}{(4\pi Dt)^{\frac{d}{2}}} e^{-st} = \frac{1}{(2\pi D)^{1-\nu}} \left(\frac{\Delta x^2}{Ds}\right)^{\frac{\nu}{2}} K_\nu\left(\Delta x\sqrt{\frac{s}{D}}\right); \tag{2.26}$$

[1] We recall the definition of the Laplace transform for a generic function $f(t)$ defined for all real values $t \geq 0$

$$\mathcal{L}\{f(t)\}(s) = \hat{f}(s) = \int_0^{+\infty} f(t)e^{-st}\, dt \tag{2.21}$$

where the complex number s is the frequency parameter. The inverse Laplace transform of $\hat{f}(s)$, if exists, is the function $f(t)$ for which $\mathcal{L}\{f\}(t) = \hat{f}(s)$. It can be proved that if $\hat{f}(s)$ has an inverse transform $f(t)$ then $f(t)$ is uniquely determined. An integral formulation of the inverse transform is given by the line integral

$$\mathcal{L}^{-1}\left\{\hat{f}(s)\right\}(t) = f(t) = \frac{1}{2\pi i} \lim_{T\to+\infty} \int_{\gamma-iT}^{\gamma+iT} \hat{f}(s)e^{st}\, dt \tag{2.22}$$

where the integration occurs along the vertical line $\Re(s) = \gamma$ in the complex plane, with γ greater than the real part of all the singularities of $\hat{f}$.

where K_m is the modified Bessel function of the second kind and $\nu = 1 - d/2$. After have inserted 2.26 in the final result of Eq. 2.23, we should perform an inverse Laplace transform in order to get a solution for the integral $I(\Delta\vec{x}, t)$, and finally an analytical expression for $p(\vec{x}_A, \vec{x}_B, t)$. Since Eq. 2.26 relies on the dimension d of the system, we may study separately the cases $d = 1$, verifying whether it gives the same results already obtained with the method of images, and $d = 2$.

2.3.1 Check for d=1

If $d = 1$ ($\nu = 1/2$) from Eq. 2.26 we obtain

$$\hat{G}_D(\Delta x, s) = \frac{1}{\sqrt{2\pi D}} \left(\frac{\Delta x^2}{Ds}\right)^{\frac{1}{4}} K_{\frac{1}{2}}\left(\Delta x \sqrt{\frac{s}{D}}\right) = \frac{e^{-\Delta x\sqrt{\frac{s}{D}}}}{2\sqrt{Ds}} \tag{2.27}$$

inserting this result in Eq. 2.25 we obtain

$$\hat{I}(\Delta x, s) = \frac{e^{-2\Delta x\sqrt{\frac{s}{2D}}}}{2\sqrt{2Ds}}; \tag{2.28}$$

and making the inverse Laplace transform

$$I(\Delta x, t) = \frac{e^{-\frac{\Delta x^2}{2Dt}}}{2\sqrt{2D\pi t}}. \tag{2.29}$$

Finally, the non-crossing probability $p(x_A, x_B|t) =: p(\Delta x, t)$ from Eq. 2.19 is

$$p(\Delta x, t) = 1 - e^{-\frac{\Delta x^2}{2Dt}} \tag{2.30}$$

that is the same result obtained with the method of images shown in Eq. 2.11; in particular it presents an asymptotic t^{-1} time dependence.

2.3.2 Calculation for d=2

Setting now $d = 2$ ($\nu = 0$) in Eq. 2.26, we obtain

$$\hat{G}_D(\Delta\vec{x}, s) = \hat{G}_D(|\Delta\vec{x}| \equiv \Delta x, s) = \frac{1}{2\pi D} K_0\left(\Delta x \sqrt{\frac{s}{D}}\right) \tag{2.31}$$

and substituting this in Eq. 2.23

$$\hat{I}(\Delta x, s) = \frac{1}{4\pi D} \frac{K_0^2\left(\Delta x\sqrt{\frac{s}{2D}}\right)}{K_0(0)} = 0 \tag{2.32}$$

since $K_0(0) = +\infty$; this implies immediately that $p(\Delta\vec{x}, t) = 1$, meaning that two DP in $d = 2$ will never exactly cross.
In order to make the intersection between polymers possible, we impose that the crossing between the two DP occurs when their distance become less than a fixed value a: this is equivalent to suppose that both polymers present a circular thickness with radius of $a/2$. The results of Eq. 2.25 should be then modified in the following way:

1. Instead of $F_{2D}(\Delta x, t)$, we are looking now for the partition function of a free directed polymer that, starting from the difference vector of the initial positions $\Delta\vec{x}$, after a time t reaches for the first time the surface of a circle of radius a centered in the origin.

2. Instead of $G_{2D}(\Delta x, t)$, we are looking now for the partition function of a free directed polymer that, starting from any point of the circumference of radius a centered in the origin, after a time t reaches $\Delta\vec{x}$.

For the point 1, it is already shown by Redner [29] that, if we consider a random-walk in d dimensions starting at $\vec{x}_0$, the Laplace transform of the probability of first reaching the surface of a sphere centered at the origin of radius a, with $x_0 > a$, in absence of other boundaries is equal to

$$\left(\frac{x_0}{a}\right)^{\nu} \frac{K_\nu\left(x_0\sqrt{\frac{s}{D}}\right)}{K_\nu\left(a\sqrt{\frac{s}{D}}\right)}; \tag{2.33}$$

setting $d = 2$ and recalling $x_0 \to \Delta x$, $D \to 2D$, we obtain exactly the Laplace transform of the partition function we need:

$$\frac{K_0\left(x_0\sqrt{\frac{s}{2D}}\right)}{K_0\left(a\sqrt{\frac{s}{2D}}\right)}. \tag{2.34}$$

The partition function described at point 2 could be instead built: taking the free propagator from a generic point $\vec{a}$ of the circumference to $\vec{x}_0$, integrating over all the

circumference, that we'll call $B_a(\vec{0})$, and normalizing for its perimeter

$$\begin{aligned}\frac{1}{2\pi a}\int_{B_a(\vec{0})} G_{2D}(\vec{a}-\Delta\vec{x},t)\,d\vec{a} &= \frac{1}{2\pi a}\int_{B_a(\vec{0})} \frac{e^{-\frac{(\vec{a}-\Delta\vec{x})^2}{8Dt}}}{8\pi Dt}\,d\vec{a} \\ &= \frac{e^{-\frac{a^2+\Delta x^2}{8Dt}}}{16\pi^2 Dt}\int_0^{2\pi} e^{\frac{2ax\cos\theta}{8Dt}}\,d\theta \\ &= \frac{e^{-\frac{a^2+\Delta x^2}{8Dt}}}{8\pi Dt} I_0\left(\frac{xa}{4Dt}\right);\end{aligned} \tag{2.35}$$

in the second passage we change the integration variable to the argument θ of the circumference, while, in the last member, I_0 is the modified Bessel function of the first kind. The Laplace transform of this expression is unknown, but in the limit $\frac{xa}{t} \to 0$ the approximation $I_0\left(xa/4Dt\right) \simeq 1$ is valid. In this way

$$\frac{1}{2\pi a}\int_{B_a(\vec{0})} G_{2D}(\vec{a}-\Delta\vec{x},t)\,d\vec{a} \;\simeq \frac{e^{-\frac{a^2+\Delta x^2}{8Dt}}}{8\pi Dt} = G_{2D}(\vec{v},t) \tag{2.36}$$

where we have defined the vector $\vec{v} = (a, \Delta x)$; its Laplace transform, according to Eq. 2.26, writes

$$\hat{G}_{2D}(\vec{v},s) = \frac{1}{4\pi D} K_0\left(\sqrt{a^2+\Delta x^2}\sqrt{\frac{s}{2D}}\right). \tag{2.37}$$

So, considering both points 1 and 2, the Laplace transform of the integral of Eq. 2.20 becomes

$$\hat{I}(\Delta x,s) = \frac{1}{4\pi D}\frac{K_0\left(\Delta x\sqrt{\frac{s}{2D}}\right) K_0\left(\sqrt{\Delta x^2+a^2}\sqrt{\frac{s}{2D}}\right)}{K_0\left(a\sqrt{\frac{s}{2D}}\right)}. \tag{2.38}$$

The inverse Laplace transform of 2.38 is impossible to calculate exactly, but since we're interested in the time asymptotic behaviour, we can study the limit $s \to 0$, that corresponds to $t \to +\infty$. The modified Bessel function K_0 for small values of the argument can be approximated to

$$K_0(z) \underset{z\to 0}{=} -\log\left(\frac{z}{2}\right) - \gamma_E + o(z^1), \tag{2.39}$$

where γ_E is the Eulero-Mascheroni constant. In this way, for $\hat{I}$ we have

$$\begin{aligned} 4\pi D\hat{I}(\Delta x, s) &\underset{s\to 0}{\approx} -\frac{\left(\log\left(\frac{\Delta x}{2}\sqrt{\frac{s}{2D}}\right)+\gamma_E\right)\left(\log\left(\frac{\sqrt{\Delta x^2+a^2}}{2}\sqrt{\frac{s}{2D}}\right)+\gamma_E\right)}{\log\left(\frac{a}{2}\sqrt{\frac{s}{2D}}\right)+\gamma_E} \\ &= -\frac{\left(\frac{1}{2}\log s + A\right)\left(\frac{1}{2}\log s + B\right)}{\frac{1}{2}\log s + C} \\ &= -\frac{\log s}{2} + C - A - B - \frac{2(A-C)(B-C)}{\log s} + o\left(\log^{-2} s\right); \end{aligned} \tag{2.40}$$

where in the first passage we have introduced the space-saving notation $A = \log \Delta x - \frac{3}{2}\log 2 - \frac{1}{2}\log D + \gamma_E$, $B = \log\sqrt{\Delta x^2 + a^2} - \frac{3}{2}\log 2 - \frac{1}{2}\log D + \gamma_E$ and $C = \log a - \frac{3}{2}\log 2 - \frac{1}{2}\log D + \gamma_E$. Since, in this asymptotic limit, the inverse of the Laplace transform of the following functions are valid [29, 31]

$$\mathcal{L}^{-1}\{\log s\}(t) \underset{s\to 0}{\approx} -\frac{1}{t}, \tag{2.41a}$$

$$\mathcal{L}^{-1}\left\{\frac{1}{\log s}\right\}(t) \underset{s\to 0}{\approx} \frac{1}{t\log^2 t}, \tag{2.41b}$$

and considered also that $\mathcal{L}^{-1}[k](t) = k\,\delta(t)$, $k \in \mathbb{R}$, the inverse Laplace transform of $\hat{I}$ for $t \to +\infty$ can be written as

$$I(\Delta x, t) \underset{t\to+\infty}{\approx} \frac{1}{4D\pi}\left(\frac{1}{2t} - \frac{2(A-C)(B-C)}{t\log^2 t}\right) \tag{2.42}$$

and finally the non-crossing probability 2.19 becomes

$$\begin{aligned} p(\Delta x, t) &\underset{t\to+\infty}{\approx} 1 - \frac{8\pi D t}{4\pi D}\left(\frac{1}{2t} - \frac{2(A-C)(B-C)}{t\log^2 t}\right) \\ &= \frac{4(A-C)(B-C)}{\log^2 t} \\ &= 2\log\frac{\Delta x}{a}\log\frac{\sqrt{\Delta x^2+a^2}}{a}\log^{-2} t \propto \log^{-2} t. \end{aligned} \tag{2.43}$$

It comes out that the non-crossing probability in $d = 2$ goes for large t as $\log^{-2} t$, showing a different behaviour from the $d = 1$ case.

2.4 Crossing probability for directed polymers in random media

In the continuum limit it is useful to introduce the non-crossing probability, $p_\eta(t)$, in the limit of near-coinciding endpoints. Namely

$$p_\eta(t) := \lim_{\epsilon\to 0} \frac{p_\eta(-\epsilon,\epsilon;-\epsilon,\epsilon|t)}{4\epsilon^2} \tag{2.44}$$

This probability depends explicitly on the disorder realization and it in general impossible to compute. However we are interested in its mean value, $\overline{p_\eta(t)}$ averaged over all disorder realizations.
In $d = 1$ we can compute $\overline{p_\eta(t)}$ explicitly by combining two properties. First, we consider the Statistical Tilt Symmetry (STS), valid for any dimension, which writes

$$\overline{\log Z_\eta(\vec{x};\vec{y}|t)} = -\frac{(\vec{x}-\vec{y})^2}{2t} + f(t), \tag{2.45}$$

where $f(t)$ is a function that does not depend on x and y. A proof for this equality is given in the Appendix A.4.
Second, as a consequence of the method of images, valid only in $d = 1$, we can express the random variable $p_\eta(t)$ as a log-derivative of the partition function

$$p_\eta(t) = \partial_x\partial_y \log Z(x;y|t)|_{\substack{x=0\\y=0}}, \tag{2.46}$$

In the Appendix A.3 we provide a proof for Equation 2.46, that belongs to a larger set of relations between non-crossing probabilities and $\log Z$ [25, 26]. Note that $\log Z$ behaves as a free energy (with opposite sign and unit temperature). By matching the two properties we get

$$\overline{p_\eta(t)} = \overline{\partial_x\partial_y \log Z(x;y|t)|_{\substack{x=0\\y=0}}} = \frac{1}{t} \tag{2.47}$$

In the free case, for which the probability is expressed by Eq. 2.10, it is easy to show that, if we set the diffusion constant at the value[2] $D = 1/2$, we have $p_{\eta\equiv 0}(t) = t^{-1}$; so there is a correspondence between the non-crossing probabilities in the free case and in the disordered case averaged over all realization of the disorder

$$\overline{p_\eta(t)} = p_{\eta\equiv 0}(t) = \frac{1}{t} \tag{2.48}$$

[2] A justification for the choice of this value is given in Section 3.1.

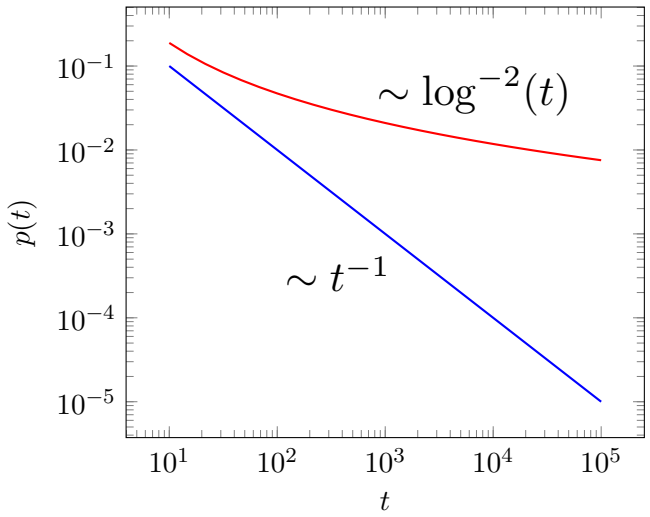

Figure 2.3: Plot of the asymptotic behaviour of the non-crossing probability $p(t)$ found for $d = 1$ in both free and disordered case (blue) and for $d = 2$ only in the free case (red).

In $d \geq 2$, Eq. 2.46 does not hold and thus the equality 2.48 should not be valid. In particular we do not know relations similar to 2.46 between the non-crossing probability and $\log Z$, that could bring to an analytical expression for $\overline{p_\eta(t)}$. So, for $d = 2$ we cannot say if the asymptotic decay in $\log^{-2} t$, found for the free case, holds also for the averaged-disordered case.

To summarize the results discussed this Chapter, in Table 2.1 we report the behaviour of the non crossing probability found out analytically in the limit of large times for every case, giving a brief summary of the methods used for each one.

Table 2.1: Behaviour of the non-crossing probability $p(t)$ in all considered cases.

Case	$p(t)$	Methods
Free case, $d = 1$	t^{-1}	Found with method of images (Section 2.2); checked using Formula 2.12 (Section 2.3.1)
Free case, $d = 2$	$\log^{-2} t$	Found using Formula 2.12 adopting results from Feller and Redner (Section 2.3.2)
Disordered case, $d = 1$	t^{-1}	Equal to the free case thanks to the STS (Section 2.4)
Disordered case, $d = 2$	?	

Chapter 3

Discrete Directed Polymers on a lattice

We now define the directed polymer on a discrete lattice. This model can be studied numerically and, in the limit of large sizes, one should recover the analytical results obtained in the continuum limit.
A discrete polymer configuration $\vec{x}(t)$ in d dimensions can be thought as a *simple random walk* on the sites $(x_1, \dots, x_d) = \vec{x}$ of the d-dimensional hypercubic lattice $\mathbb{Z}^d$ [30]; this means that, at each step, the particle can only jump to neighboring sites of the lattice, according to some probability distribution. A jump from a site to another among the $2d$ nearest neighbours is then performed in correspondence of a "jump" forward in the discrete time interval {0,1,2,...,t}; in this way, the growth of the polymer for the $(\tau+1)$-th step can be generally written as

$$\vec{x}(\tau+1) = \vec{x}(\tau) \pm e_j = \begin{pmatrix} x_1(\tau) \\ x_2(\tau) \\ \vdots \\ x_j(\tau) \\ \vdots \\ x_d(\tau) \end{pmatrix} \pm \begin{pmatrix} 0 \\ 0 \\ \vdots \\ 1 \\ \vdots \\ 0 \end{pmatrix} \ , \ j \in \{1, 2, \dots, d\} \tag{3.1}$$

Let's distinguish then between the free directed polymers and directed polymers in disordered media, as done in the previous Chapter.

- A free directed polymer on a lattice is equivalent to a *symmetric simple random*

walk, for which the probabilities of the particle jumping to each one of its nearest neighbors are the same. This means, in particular, that every polymer configuration starting from a certain point $\vec{x}$ and ending at $\vec{y}$ has the same probability of occurring.

- For a directed polymer in a disordered medium, each point of the $(d+1)$-dimensional discrete space $(\vec{x}, \tau)$ is associated with a local random energy $\eta(\vec{x}, \tau)$ that obeys to Eq. 2.4. Given a realization of the random energy for every site, the energy of a directed polymer starting and ending at time 0 and t respectively is then the sum of the energies associated with the sites crossed by the polymer in the time interval $0 \leq \tau \leq t$.

$$E\left[\vec{x}(t)\right] = \sum_{\tau=0}^{t} \eta(\vec{x}, \tau) \tag{3.2}$$

  At finite temperature T the probability of a given configuration is proportional to $\exp[-\beta E\left[\vec{x}(t)\right]$, while at zero temperature the Boltzmann measure is concentrated on the polymer that minimizes the energy, that we call 'ground state' of the system.
  .

The boundary conditions of the problem, i.e. the starting and the final point of the polymer, should be specified; here we are interested in the so-called *droplet initial conditions*, for which $\vec{x}(0) = \vec{x}(t)$. Let's consider then two polymers $\vec{x}_A(t)$ and $\vec{x}_B(t)$, with droplet initial conditions $\vec{x}_A(0) = \vec{x}_A(t) = \vec{x}_A$ and $\vec{x}_B(0) = \vec{x}_B(t) = \vec{x}_B$. We want to determine the probability $p(\vec{x}_A, \vec{x}_B, t)$ that they cross at least once when $0 < \tau < t$,and in particular we are interested in its asymptotic behaviour for large t. In particular in the disordered case, we are interested in the non-crossing probability between two ground states, averaged over all realizations of the disorder.

3.1 Free case: Matching discrete with continuous

Consider the symmetric simple random walk for $d = 1$; for each time, the particle could either take one step in the positive direction (increasing its position value by 1) or in the negative direction (decreasing by 1) equivalently, with the same probability of 1/2. We're looking for the probability $P(\Delta x, t)$ that, after t steps, the particle arrives at a distance Δx from the initial site. This means that $m = (t + \Delta x)/2$ steps are taken in the positive direction; the probability $P(m, t)$, that among t steps m are positive (for

instance), is given by the binomial distribution

$$P(m,t) = \left(\frac{1}{2}\right)^m \left(\frac{1}{2}\right)^{t-m} \binom{t}{m} = \frac{1}{2^t} \frac{t!}{m!(t-m)!}. \tag{3.3}$$

If we take the logarithm, using the Stirling approximation $\log x! \approx x \log x - x$ valid for $x >> 1$, neglecting the term $1/2^t$ since it is part of the normalization that we will calculate at the end, we have

$$\begin{aligned} \log P(m,t) &\approx t \log t - t - m \log m + m - (t-m)\log(t-m) + t - m \\ &= t \log t - m \log m - (t-m)\log(t-m) \end{aligned} \tag{3.4}$$

Now we approximate $\log P(m,t)$ around its maximum, located at $m = m^*$, using a Taylor series at the second order:

$$\log P(m,t) \approx \log P(m^*,t) + \frac{1}{2} \frac{\partial^2 \log P(m,t)}{\partial m^2}\bigg|_{m=m^*} (m-m^*)^2. \tag{3.5}$$

Imposing the condition to the derivative with respect to m of $\log P(m,t)$

$$\frac{\partial \log P(m,t)}{\partial m}\bigg|_{m=m^*} = \log\left(\frac{t-m^*}{m^*}\right) \stackrel{!}{=} 0, \tag{3.6}$$

we find $m^* = t/2$; so the second derivative of $\log P(m,t)$ at $t/2$ gives

$$\frac{\partial^2 \log P(m,t)}{\partial m^2}\bigg|_{m=\frac{t}{2}} = \left(-\frac{1}{m} - \frac{1}{t-m}\right)\bigg|_{m=\frac{t}{2}} = -\frac{4}{t}; \tag{3.7}$$

we thus find the explicit form for 3.5, and then the expression for $P(m,t)$ valid for $t >> 1$

$$\log P(m,t) = A(t) - \frac{2}{n}\left(m - \frac{t}{2}\right)^2 \implies P(m,t) = B(t)\, e^{-\frac{2}{t}\left(m-\frac{t}{2}\right)^2} \tag{3.8}$$

where $A(t)$ and $B(t)$ are constant with respect to m; with the variable change $\Delta x = 2m - t$, imposing the unitary normalization condition, we find

$$P(\Delta x, t) = \frac{e^{-\frac{\Delta x^2}{2t}}}{\sqrt{2\pi t}}. \tag{3.9}$$

For $d > 1$, since there is no correlation between the d components of the particle's motion along the d dimensions, the probability that, after t steps, the particle is situated at the

distance $\Delta\vec{x} = (\Delta x_1, \ldots, \Delta x_d)$ from the initial site is

$$P(\Delta\vec{x}, t) = \frac{e^{-\frac{\Delta x_1^2}{2t}}}{\sqrt{2\pi t}} \ldots \frac{e^{-\frac{\Delta x_d^2}{2t}}}{\sqrt{2\pi t}} = \frac{e^{-\frac{\Delta x^2}{2t}}}{(2\pi t)^{\frac{d}{2}}}, \tag{3.10}$$

that is exactly equal to Eq. 2.3, the partition function of a free directed polymer in d dimensions in the continuous limit, if we set $D = 1/2$. So, starting from the symmetric simple random walk and taking $t \to +\infty$, we find the problem of free directed polymer in the continuous limit already illustrated in the previous Chapter. Moreover, this justifies the choice for D made in Section 2.4.

3.2 Algorithms

In this Section we illustrate the structure of the algorithms implemented for the creation of directed polymers with droplet boundary conditions, for both free and disordered cases and for both $d = 1$ and $d = 2$.

3.2.1 Algorithms for the Free case

The operations performed in the algorithm for $d = 1$ and $d = 2$ are both listed in Table 3.1. Here we discuss some peculiarities of the two different dimensions.

- $\boldsymbol{d = 1}$. Supposing a polymer that start at $x(0)$ and ends at $x(t)$, it is easy to show that, calling $\Delta x = x(t) - x(0)$, $(t + \Delta x)/2$ steps will necessary take place in the positive direction, while the other $(t - \Delta x)/2$ in the negative; in particular if $x(t) = x(0)$, the number of steps in the positive and in the negative direction are the same, namely $t/2$.

- $\boldsymbol{d = 2}$. Since $\mathbb{R}^2 \simeq \mathbb{C}$, we can express the position of the polymer on the $\mathbb{Z}^2$ lattice as a complex number: a jump along the real axis will cause an increase/decrease of the position by 1, while a jump along the complex axis will cause an increase/decrease of the position by i.
  As for $d = 1$, if the initial and the final point are the same, the number of leaps taken in a direction and in the opposite one, along a certain axis, must be equal; so, if the polymer is t steps long, the number of pairs of opposite jumps is still $t/2$. However now, in order to build a polymer we have to choose the number n of pairs of opposite steps that will perform along one of the two axis, so that

Free case, $d = 1$

Operations	**Example for $t = 8$**
• Initial conditions for Poly;	Poly[0] = 0, Poly[8] = 0;
• Initialization of Step;	Step = $[1, -1, 1, -1, 1, -1, 1, -1]$;
• Random permutation of Step;	Step = $[-1, -1, 1, 1, 1, -1, 1, -1]$;
• Creation of Poly: for $\tau = 0, 1, \ldots, t-1$: Poly$[\tau+1]$ = Poly$[\tau]$ + Step$[\tau]$;	Poly[1] = Poly[0] + Step[0] = -1; Poly[2] = Poly[1] + Step[1] = -2; $\ldots$
Final result for Poly:	Poly = $[0, -1, -2, -1, 0, 1, 0, 1, 0]$;

Free case, $d = 2$

Operations	**Example for $t = 8$**
• Initial conditions for Poly;	Poly[0] = 0, Poly[8] = 0;
• Sampling and rounding of n;	$n = 2.7 \rightarrow \text{Round}(n) = 3$
• Initialization of Step;	Step = $[1, -1, 1, -1, 1, -1, i, -i]$;
• Random permutation of Step;	Step = $[-1, -i, 1, -1, 1, i, 1, -1]$;
• Creation of Poly: for $\tau = 0, 1, \ldots, t-1$: Poly$[\tau+1]$ = Poly$[\tau]$ + Step$[\tau]$;	Poly[1] = Poly[0] + Step[0] = -1; Poly[2] = Poly[1] + Step[1] = $-1-i$; $\ldots$
Final result for Poly:	Poly = $[0, -1, -1-i, -i, -1-i, -1, 0, 1, 0]$;

Table 3.1: Schemes of the algorithms adopted for creating a Free directed polymer on a lattice in $d = 1$ (top) and $d = 2$ (bottom). 'Poly' is an array with $t + 1$ entrances representing the polymer, for which the τ-th entrance Poly$[\tau]$ is its position at time τ, while 'Step' is an array that collects the t leaps that the polymer has to perform. All the operations, listed on the left, are accompanied by an example, illustrated on the right.

the number of pairs along the other will be $t/2 - n$; The total number $N(n,t)$ of possible configurations of a polymer presenting n pairs along the real axis (for instance) is given by the permutation of t elements among which n couples and $t/2 - n$ couples are respectively identical between them

$$N(n,t) = \frac{t!}{(t/2-n)!^2\, n!^2}. \tag{3.11}$$

In order then to find the probability $P(n,t)$ that a polymer presents n pairs along the real axis in the limit $t \to +\infty$, we perform a calculation analogous to the one shown in Section 3.1. The natural logarithm of $N(n,t)$ for $t >> 1$ could be written as

$$\log N(n,t) = t\log t - 2\left(\frac{t}{2}-n\right)\log\left(\frac{t}{2}-n\right) - 2n\log n \tag{3.12}$$

imposing that the derivative with respect to n at the maximum point n^* is 0, gives

$$\left.\frac{\partial \log N(n,t)}{\partial n}\right|_{n=n^*} = \left.\log\left(\frac{t/2-n}{n}\right)\right|_{n=n^*} \stackrel{!}{=} 0 \implies n^* = \frac{t}{4}; \tag{3.13}$$

the second derivative at $n^* = t/4$ is

$$\left.\frac{\partial^2 \log N(n,t)}{\partial n^2}\right|_{n=\frac{t}{4}} = \left.-\frac{t}{n\left(\frac{t}{4}-n\right)}\right|_{m=\frac{t}{4}} = -\frac{16}{t}, \tag{3.14}$$

so, near n^*, $\log N(n,t)$ can be approximated to

$$\begin{aligned}\log N(n,t) &\approx \log N(n^*,t) + \frac{1}{2}\left.\frac{\partial^2 \log N(n,t)}{\partial n^2}\right|_{n=n^*}(n-n^*)^2 \\ &= A(t) - \frac{8}{t}\left(n-\frac{t}{4}\right)^2;\end{aligned} \tag{3.15}$$

the probability $P(n,t)$, with the proper normalization factor, is then

$$P(n,t) = \sqrt{\frac{\pi t}{8}}\, e^{-\frac{8(n-t/4)^2}{t}}, \tag{3.16}$$

namely a Gaussian with mean and variance both equal to $t/4$. In order to build a 2-dimensional free directed polymer, the algorithm should then sample the number n of pairs of leaps in the distribution $\mathcal{N}(t/4, t/4)$ and round it to an integer.

3.2.2 Algorithms for the Disordered case: Dijkstra's algorithm

In presence of disorder the polymer configurations are not equally likely, and at zero temperature only the polymer with the minimal energy is occupied. In order to find the ground state given the initial and final points in a system of size t, one can calculate the energies of all the $(2d)^t$ possible configurations, summing the energies of the crossed sites as expected from Equation 3.2, and then find the minimum among them; however, the running time of the entire operation explodes for t sufficiently large, since the total number of operations grows as a power of t. For this purpose, we decide instead to implement a variant of the Dijkstra's algorithm. In its original formulation [32] this algorithm allows to find the path of minimal length connecting two points of a generic graph. The Dijkstra algorithm is the basic ingredient of all the shortest path-finding algorithms [33].
In our case the graph is the directed $(d+1)$-dimensional lattice, and the path of minimal length is the ground state polymer. Hence, each site of the lattice $(\vec{x}, \tau)$ has $2d$ directed edges that point on $(\vec{x}_{\text{n.n.}}, \tau + 1)$, where $\vec{x}_{\text{n.n.}}$ indicates one of the $2d$ nearest neighbours of $\vec{x}$. The length of the edge connecting $(\vec{x}, \tau)$ to $(\vec{x}_{\text{n.n.}}, \tau + 1)$ is $\eta(\vec{x}_{\text{n.n.}}, \tau + 1)$, namely the random energy assigned to $(\vec{x}_{\text{n.n.}}, \tau+1)$; so the length of a path is actually the energy of the correspondent directed polymer.
Considered then the particular structure of our graph, we build an algorithm that allows us, given the initial and final points of the polymer, to find the ground state of the system, returning an array that collects its position at every time from 0 to t, and its energy E_0. The operations implemented for $d = 1$ are listed in Table 3.2 in the form of pseudo-code and applied to an example, which is also graphically illustrated in the Figures 3.1 and 3.2, while the operations for $d = 2$ are listed in Table 3.2; here we explain better some of the points listed:

- **Initialization of E and Dis**: all the entrances of the d-dimensional array 'E' are set to a value N sufficiently larger than the typical energy values provided by the probability distribution that generates the disorder, except one entrance which is set to 0; the position of the 0 entrance along the array represents the initial x-position of the polymer at $\tau = 0$, as shown, for $d = 1$, on the top left of Figure 3.1. Moreover, a set of random values is created and stored in the 'Dis' array, representing the energies assigned to the nodes of our graph, always shown in Figure 3.1 for $d = 1$; the number of entrances of this array is then equal to the number of sites of the lattice. For all the simulation performed, we choose to generate the random values from a Gaussian distribution of mean 0 and variance 1.

Disordered case, $d = 1$

Operations	**Example for $t = 4$**
• Initialization of E and Dis; for $x = -t/2 - 1,\ -t/2,\ \ldots,\ t/2 + 1$: $\mathrm{E}[x] = \begin{cases} 0 & \text{if } x = 0 \\ N & \text{else} \end{cases}$;	$\mathrm{E} = [N, N, N, 0, N, N, N]$;
$\mathrm{Dis} = [\eta_1,\ \eta_2,\ \ldots]$;	$\mathrm{Dis} = [-0.5, 1.6, \ldots, -1.2]$;
• Update of E and Step: for $\tau = 1, 2, \ldots, t/2$: for $x = -\tau, -\tau + 2, \ldots, \tau$: $\mathrm{E}[x] = \min\{E[x-1], E[x+1]\} + \mathrm{Dis}[j]$; $\mathrm{Step}[\tau][x] = \begin{cases} +1 & \text{if min} = E[x+1] \\ -1 & \text{if min} = E[x-1] \end{cases}$; $j = j + 1$;	$\tau = 1,\ x = -1$: $\mathrm{E}[-1] = \min\{E[-2], E[0]\} + \mathrm{Dis}[1]$; $= 0 - 0.5 = -0.5$; $\mathrm{Step}[-1][1] = -1$; $\tau = 1,\ x = 1$: $\mathrm{E}[1] = \min\{E[0], E[2]\} + \mathrm{Dis}[2] = 1.6$; $\mathrm{Step}[1][1] = 1$;
for $\tau = t/2 + 1, t/2 + 2, \ldots, t$: for $x = \tau - t, \tau - t + 2, \ldots, -\tau + t$: $\mathrm{E}[x] = \min\{E[x-1], E[x+1]\} + \mathrm{Dis}[j]$; $\mathrm{Step}[\tau][x] = \begin{cases} +1 & \text{if min} = E[x+1] \\ -1 & \text{if min} = E[x-1] \end{cases}$; $j = j + 1$;	$\ldots$
• Set final position of Poly; $\mathrm{Poly}[t] = 0$;	$\mathrm{Poly}[4] = 0$;
• Creation of Poly: for $\tau = 1, 2, \ldots, t$ $\mathrm{Poly}[t - \tau] = \mathrm{Poly}[t - \tau + 1] +$ $+\mathrm{Step}[t - \tau + 1][\mathrm{Poly}[t - \tau + 1]]$;	$\mathrm{Poly}[3] = \mathrm{Poly}[0] + \mathrm{Step}[4][0] = -1$; $\mathrm{Poly}[2] = \mathrm{Poly}[1] + \mathrm{Step}[3][-1] = 0$; $\ldots$
Final result for Poly:	$\mathrm{Poly} = [0, -1, 0, -1, 0]$, $E_0 = -0.9$;

Table 3.2: Scheme of the algorithm adopted for creating a directed polymer on a disordered lattice in $d = 1$. 'Poly' is an array with $t + 1$ entrances representing the polymer, for which the τ-th entrance Poly[τ] is its position at time τ, while 'Step' is a 2-dimensional array that collects the leaps that the polymer has to perform.

Disordered case, $d = 2$

Operations

- Initialization of E and Dis;
  for $x = -t/2 - 1, -t/2, \ldots, t/2 + 1$:
    for $y = -t/2 - 1, -t/2, \ldots, t/2 + 1$:
      $$\mathrm{E}[x][y] = \begin{cases} 0 & \text{if } x = y = 0 \\ N & \text{else} \end{cases} ;$$
  $\mathrm{Dis} = [\eta_1, \eta_2, \ldots]$;

- Update of E and Step:
  for $\tau = 1, 2, \ldots, t/2$:
    for $x = -\tau, -\tau + 1, \ldots, \tau$:
      for $y = -\tau + |x|, -\tau + |x| + 2, \ldots, \tau - |x|$:
      $\mathrm{E}[x][y] = \min\{\mathrm{E}[x-1][y], \mathrm{E}[x+1][y], \mathrm{E}[x][y-1], \mathrm{E}[x][y+1]\} + \mathrm{Dis}[j]$;
      $$\mathrm{Step}[x][y][\tau] = \begin{cases} (\pm 1, 0) & \text{if } \min = E[x \pm 1][y] \\ (0, \pm 1) & \text{if } \min = E[x][y \pm 1] \end{cases} ;$$
      $j = j + 1$;

  for $\tau = t/2 + 1, t/2 + 2, \ldots, t$:
    for $x = \tau - t, \tau - t + 1, \ldots, -\tau + t$:
      for $y = \tau - t + |x|, \tau - t + |x| + 2, \ldots, t - \tau - |x|$:
      $\mathrm{E}[x][y] = \min\{\mathrm{E}[x-1][y], \mathrm{E}[x+1][y], \mathrm{E}[x][y-1], \mathrm{E}[x][y+1]\} + \mathrm{Dis}[j]$;
      $$\mathrm{Step}[x][y][\tau] = \begin{cases} (\pm 1, 0) & \text{if } \min = E[x \pm 1][y] \\ (0, \pm 1) & \text{if } \min = E[x][y \pm 1] \end{cases} ;$$
      $j = j + 1$;

- Set final position of Poly;
  $\mathrm{Poly}[t] = (0, 0)$;

- Creation of Poly:
  for $\tau = 1, 2, \ldots, t$
    $\mathrm{Poly}[t - \tau] = \mathrm{Poly}[t - \tau + 1] + \mathrm{Step}[t - \tau + 1][\mathrm{Poly}[t - \tau + 1]]$;

Table 3.3: Scheme of the algorithm adopted for creating a directed polymer on a disordered lattice in $d = 2$. 'Poly' is an array with $t + 1$ entrances representing the polymer, for which the τ-th entrance $\mathrm{Poly}[\tau]$ is its position at time τ, while 'Step' is a 2-dimensional array that collects the leaps that the polymer has to perform.

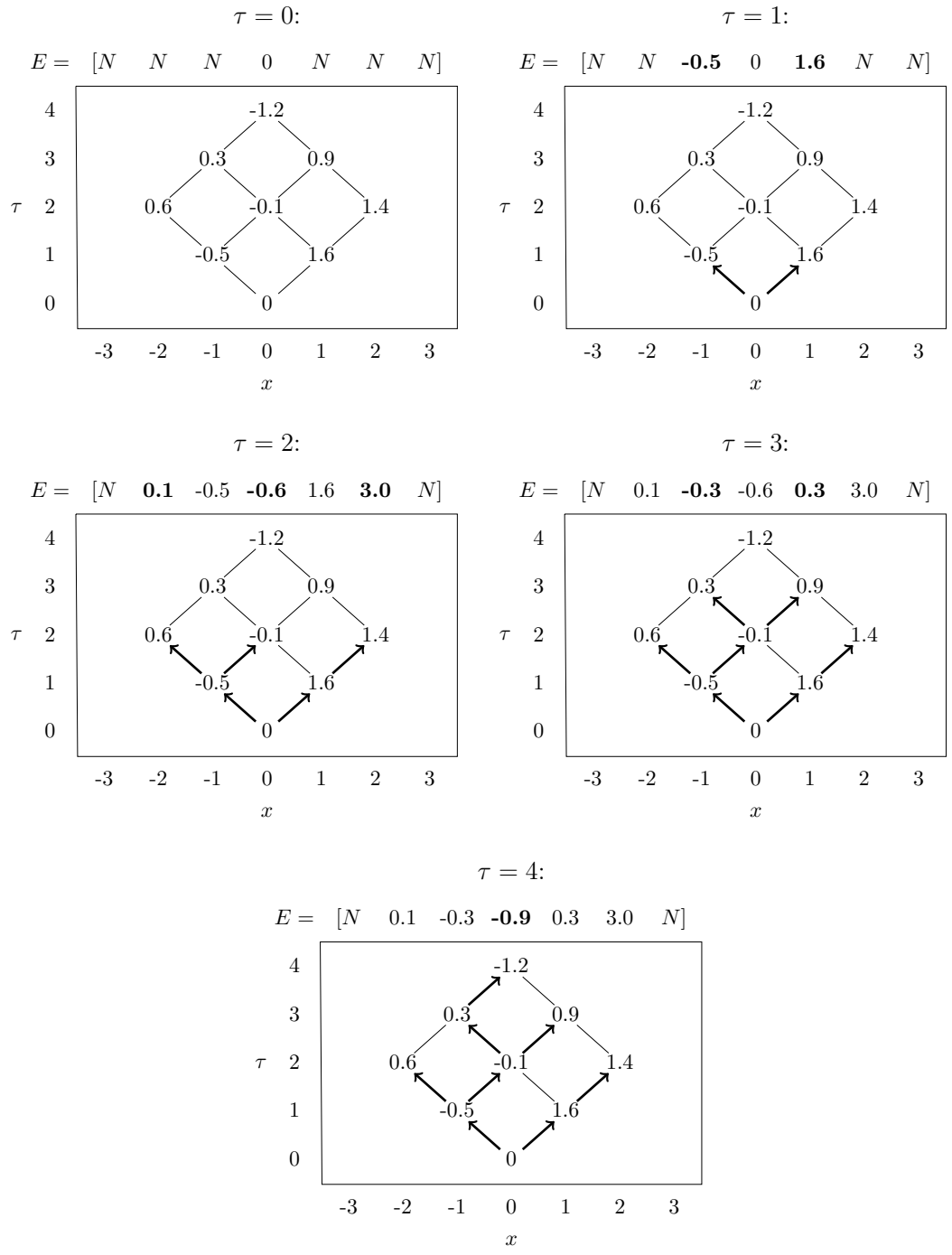

Figure 3.1: Graphical representation of the update of the energy array 'E' described in the second point of Table 3.2. The updated entrances of 'E' for a certain τ are evidenced in bold; everyone of them corresponds to the sum of all the energy values, shown in the graphs, crossed by the path that, starting from the initial site at $\tau = 0$ and following the arrows, arrives at the site with same x-position at that time τ. In particular, the energy value E[0] at $\tau = 4$ corresponds to the energy E_0 of the ground state.

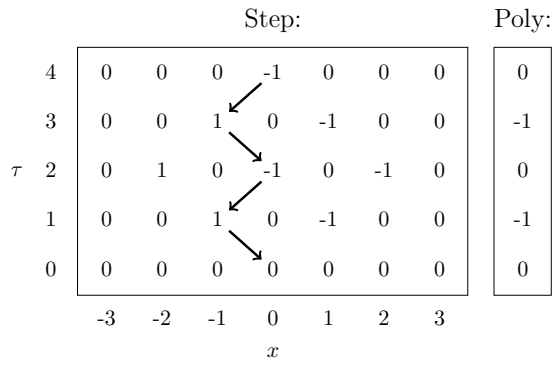

Figure 3.2: Graphical representation of the update of the array Poly described in the last point of Table 3.2. The arrows evidence the values of the Step array chosen by the ground state polymer.

Note that we are free to choose any distribution: the only condition is to generate uncorrelated random values.

- **Update of E and Step**: For every j-th node of the $(d+1)$-dimensional lattice in which the ground state may move, illustrated for $d = 1$ in Figure 3.1, an entrance of 'E' is updated and a new entrance of Step is filled with a new value, following respectively the operation

$$\mathrm{E}[x_1][x_2]\dots[x_d] = \min_{i\in \mathrm{n.n.}} \{\mathrm{E}[x_{1,i}][x_{2,i}]\dots[x_{d,i}]\} + \mathrm{Dis}[j];$$

$$\mathrm{Step}[\tau][x_1]\dots[x_d] = \pm e_k \text{ if } \min = \mathrm{E}[x_1][x_2]\dots[x_k \pm 1]\dots[x_d];$$

  where $e_k = (0, \dots, 1, \dots, 0)$, with the non-null entrance at the k-th position.

- **Creation of Poly**: the algorithm for the update of the 'Poly' array is basically the same of the free case, previously shown in Table 3.1, but now Step is a $(d+1)$-dimensional array, and, from a graphic point of view, the entrances selected step by step forms the path of the ground state, as shown for $d = 1$ in Figure 3.1.

If we analyze the running time of this algorithm, the most complex part is represented by the updating of 'E' and 'Step', which is repeated for a number of times equal to the number of nodes of our $(d + 1)$-dimensional graph. The total amount of sites can be estimated summing the number of sites at a certain τ for every τ from 1 to $t/2$, observing that this number increases as a power of d in this interval, and then multiplying by 2 in

order to count the remaining sites from $t/2+1$ to t:

$$\#\text{ sites } \simeq 2\sum_{\tau=1}^{t/2}\tau^d = 2H_{\frac{t}{2},-d} \propto t^{d+1}, \tag{3.17}$$

where $H_{\frac{t}{2},-d}$ is the generalized harmonic number of order $-d$ of $t/2$. Considering that $t^{d+1} << (2d)^t$ for large t, this variant of the Dijkstra's algorithm is actually faster than the straightforward procedure described at the beginning of this Section.

3.3 Numerical results

3.3.1 Results for the non-crossing probability

In order to generate two polymers A and B with droplet boundary conditions, that starts (and ends) at two different positions separated by a distance Δx, we adopt the algorithms just explained in the previous Section, considering that:

- For the free case, we generate the Steps array for the two polymers with the same method, but, for the creation of the Poly arrays, we set different initial and final positions, assuring that their difference value is Δx;
- For the disordered case, in order to update the two energy arrays related to the two different polymers, we use the same 'Dis' array filled with the same random values, but the entrances used for the polymer A are shifted with respect to the ones used for the polymer B; if we call $\mathrm{E_A}$ and $\mathrm{E_B}$ the energy vectors for the polymers A and B respectively, we will have:

$$\begin{aligned}&\mathrm{E_A}[x_1][x_2]\dots[x_d] = \min_{i\in\text{n.n.}}\{\mathrm{E}[x_{1,i}][x_{2,i}]\dots[x_{d,i}]\} + \mathrm{Dis}[j];\\ &\mathrm{E_B}[x_1][x_2]\dots[x_d] = \min_{i\in\text{n.n.}}\{\mathrm{E}[x_{1,i}][x_{2,i}]\dots[x_{d,i}]\} + \mathrm{Dis}[j+\Delta x/2];\end{aligned} \tag{3.18}$$

  then, as for the free case, we set different initial and final positions for the two polymers;

For every considered case, in order then to estimate the non-crossing probability $p(t)$ between two polymers of fixed length t

1. We generate a collection of different pairs of polymers, running the algorithm the number of times desired; in the disordered cases, the realization of the disorder

must be changed every time, meaning that the values in the 'Dis' array must be discarded and substituted with other random values.

2. Among the couples generated, for $d = 1$ we count the ones for which the two polymers never occupy the same position at the same time, while for $d = 2$ we count the ones for which the two polymers are never located at a distance less then or equal to a fixed value a, where $a < x$ (see Subsection 2.3.2); the ratio between the number of couples counted in this way and the number of total couples generated gives an estimation of $p(t)$.

Checking whether two directed polymers cross or not is equivalent to sampling a random variable which, for a fixed t, has a Bernoulli distribution

$$f(k) = \begin{cases} 1 - p(t) \text{ if } k = 0 \\ p(t) \quad \text{if } k = 1 \end{cases} \tag{3.19}$$

for which the variance is equal to $p(t)(1 - p(t))$. So, the estimation of $p(t)$ obtained averaging over N_s sampling of the variable has an error equal to

$$\sigma_{p(t)} = \sqrt{\frac{p(t)(1-p(t))}{N_s}} \simeq \sqrt{\frac{p(t)}{N_s}}. \tag{3.20}$$

The error for every estimation of $p(t)$ performed was then calculated using Equation 3.20.

In Figure 3.3 and 3.4 we plot in a logarithmic scale the results obtained for $d = 1$ and $d = 2$ respectively. For $d = 1$ the asymptotic t^{-1} behaviour is found for both free and disordered case, confirming the analytical result $p_{\eta\equiv 0}(t) = \overline{p_\eta(t)}$. For $d = 2$, in the free case we found that $p(t)$ scales as a logarithmic power law, and for large t the predicted limit $p(t) \sim \log^{-2} t$ is approached. In the disordered case, $p(t)$ show instead a particular behaviour, since it seems to scale as a power law which exponent is not constant but slightly increase as t becomes larger; for the set of data collected, we can only infer that $p(t) \sim t^{-\alpha}$ with $0.5 \lesssim \alpha \lesssim 0.75$. Hence, according to our numerical simulations, the match between the free and the disordered case does not occur for $d = 2$.
In Table 3.4 we summarize the numerical results obtained, the algorithm developed to obtain them and the order of magnitude of their computational cost.

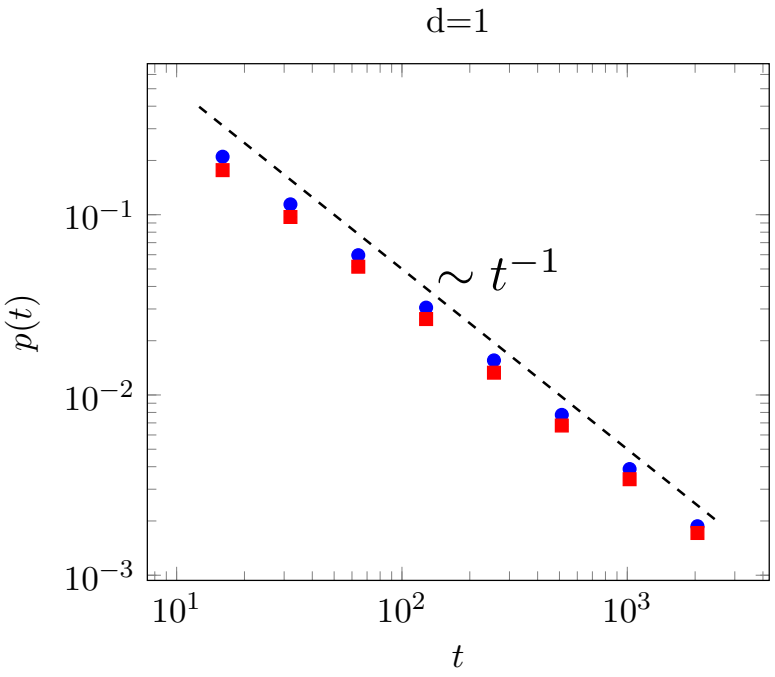

Figure 3.3: Plot of the non-crossing probability $p(t)$ in $d = 1$ for $t = 2^n$, $n = 4, \ldots, 11$, distinguishing the free case (indicated with blue circles) from the disordered case (red squares). Every value was obtained setting $\Delta x = 2$ and sampling 10^6 couples of polymers.

Table 3.4: Behaviour of the non-crossing probability $p(t)$.

	$d = 1$	$d = 2$	Algorithms	Cost
Free case	t^{-1}	$\log^{-2}(t)$	Random permutation of array with equal # steps in opposite directions	$O(t)$
Disordered case	t^{-1}	$t^{-\alpha}$, $0.5 \lesssim \alpha \lesssim 0.75$	Variant of Dijkstra's algorithm to find the minimal path	$O(t^{d+1})$

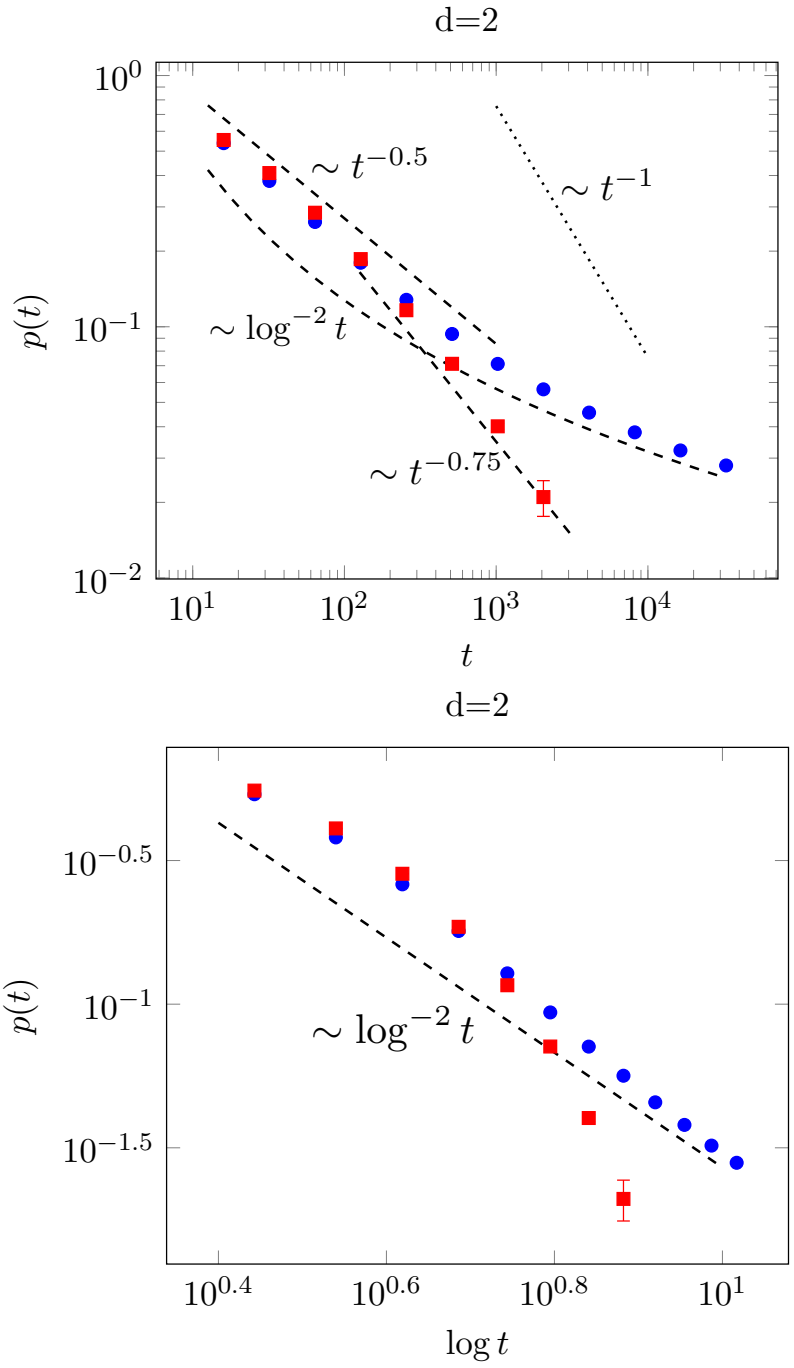

Figure 3.4: Plot of the non-crossing probability $p(t)$ in $d = 2$ for $t = 2^n$, $n = 4, \ldots, 15$, distinguishing the free case (indicated with blue circles) from the disordered case (red squares). Upper: Plot of $(t, p(t))$. Lower: Plot of $(\log t, p(t))$. Every value was obtained setting $\Delta x = 4$ and $a = 2$, while the number of sampling for every t considered varies from $\sim 10^3$ to 10^6.

3.3.2 Results for the energy gap distribution

To confirm the estimations of the non-crossing probability in the disordered case, we also try to estimate, for both $d = 1, 2$ and different values of t, the distribution $\rho_t(\delta E)$ of the energy gap δE for $\delta E \to 0$ between a ground state and its first excited starting and ending at the same points, verifying whether $\rho_t(\delta E \to 0)$ scales as the averaged-disordered non-crossing probability $\overline{p_\eta(t)}$ as explained in Section 1.4.2.
In this case, in order to calculate the energy gap of a couple of polymer:

1. We generate the ground state polymer thanks to the algorithm for the disordered case (Table 3.2 and 3.3 respectively for $d = 1$ and $d = 2$), obtaining its energy E_0.
2. We create the first excited polymer starting and ending at the same points, but making sure that it doesn't occupy, for every $\tau = 1, \dots, t-1$, the same position occupied by the ground state at that τ. This was possible using the same algorithm and adopting the same realization of the disorder used for building the ground state, with the modification that, for every $\tau = 1, \dots, t-1$, after all the updates of the array 'E' and 'Step' provided for that value of τ, we set E[Poly[τ]] $= N$, where N is sufficiently larger than the typical energy values provided by the distribution that generates the disorder. In this way the second polymer will not grow where the first has passed before: the path corresponding to the first excited is the second energetic minimal path. We obtain then its energy E_1.
3. The energy gap is thus the difference between the energy of the first excited and the one of the ground state, namely $\delta E = E_1 - E_0$.

In Figures 3.5 and 3.6 we collect in a histogram the values of energy gaps calculated sampling several pairs of polymers, obtaining a reconstruction of $\rho_t(\delta E)$ for different values of t. The distributions are then rescaled for t and $t^{0.7}$ respectively in the $d = 1$ and $d = 2$ case; if the rescaled distributions occur at the same height in the limit $\delta E \to 0$, it means that $\rho_t(\delta E \to 0)$ scales as $\overline{p_\eta(t)}$. For $d = 2$ the exponent 0.7 was chosen since, for the four values of t considered, the correspondent estimations of the non-crossing probability seem fitted well by a power law with that exponent (see Figure 3.4). It comes out that, in both dimensions, the energy gap distribution for small δE scales with the same power law as $\overline{p_\eta(t)}$, verifying numerically the relation discussed in Section 1.4.2.

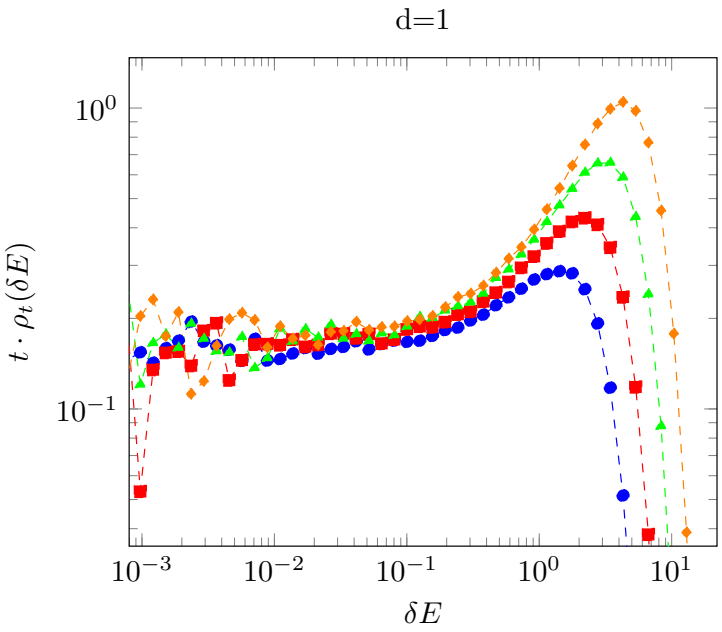

Figure 3.5: Plot of the rescaled distributions $\rho_t(\delta E)$ in $d = 1$ for $t = 2^n$,$n = 5, 6, 7, 8$, indicated respectively by circles, squares, triangles and diamonds. For every t, 10^6 values of δE were sampled.

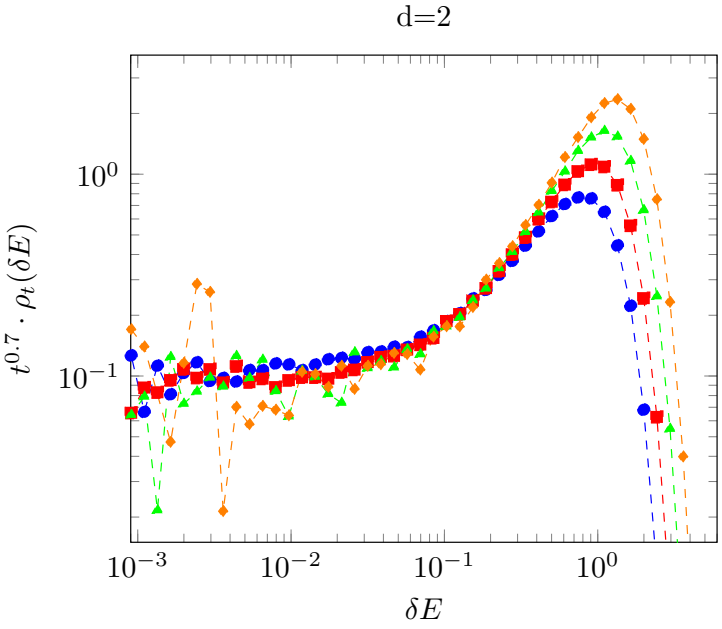

Figure 3.6: Plot of the rescaled distributions $\rho_t(\delta E)$ in $d = 2$ for $t = 2^n$,$n = 5, 6, 7, 8$, indicated respectively by circles, squares, triangles and diamonds. 10^6 values of δE were sampled for $t = 2^5$ and 2^6, while $\sim 4 \cdot 10^5$ were sampled for $t = 2^7$ and $\sim 2.5 \cdot 10^5$ for $t = 2^8$.

Chapter 4

Conclusions and Perspectives

In this thesis we studied both analytically and numerically the non-crossing probability of two directed polymer in both cases of presence and absence of disorder and in both (1+1) and (2+1) dimensions. In dimension (1+1) we found the results already predicted in previous works [25], while in dimension $(2+1)$ we calculate exactly the free case in the limit of long polymers and found that the probability goes to 0 as $1/\log^2 t$ with t the size of the polymer, which appears to be an original result. In the disordered case we performed numerical simulations adapting the Dijkstra's algoritm to our model, and in $(2+1)$ dimension we found a power-law decay $t^{-\alpha}$ slower than in dimension $(1+1)$, but faster than in the same dimension in absence of disorder. Due to time constraints we stop our simulation at $t = 2^{12}$, but it would be interesting to collect data for higher sizes of the system, in order to obtain a more precise estimation of α in the asymptotic limit $t \to +\infty$.
The original purpose of this thesis was to study an equivalent of the Darcy law for a non-Newtonian fluid in a 3-dimensional porous medium. In particular, for a Bingham plastic the flow becomes different from zero over a critical pressure value P_0 following a non-linear behaviour $Q \propto (P - P_0)^\beta$ with $\beta > 1$: this corresponds to a phase transition, for which one expects scale free behaviour, that were observed numerically in 2 dimension [17]. Our results confirm the presence of divergent length scales also in 3 dimensions.

Regarding the study of the Darcy rheology, one of the problems that remains to be solved is to connect the behaviour of the flow curve with the geometrical properties of the open channels. For example, it would be very worthwhile to find a scaling relation between the exponents β and α already discussed. Another question of relevant practical importance

is the interaction between a yield stress fluid and a Newtonian fluid that both flow in a porous medium; a possible research should concentrate in studying the geometry of the interface between the two different materials, investigating the phenomenon of "fingerization", for which the Newtonian fluid breaks through the non-Newtonian one in the form of highly branched channels patterns [14].
If we look instead at the problem itself of directed polymers, it would be interesting to study the non-crossing probability for higher dimensions, verifying if the two polymers never cross with a finite probability as predicted for the free case by the Pólya's theorem [19].

4.1 Statistics of the overlap

The methods developed in this thesis allow to compute the statistical distribution of the overlap's lenght of two ground states starting and ending at near coinciding points.
Considering two directed polymers of lenght t in the continuum limit, in $d = 1$ dimension it is possible to show that, for a fixed realization of the disorder η, the probability density $P(\tau)$ that their first crossing occurs at time $\tau \in]0, t[$ writes

$$P(\tau) = \frac{\int_{-\infty}^{+\infty} dz\, Z_\eta^2(0; z|\tau)\, Z_\eta^2(z; 0|t-\tau)\, \partial_x \partial_y \log Z(x; y|\tau)|_{x=0, y=z}}{Z_\eta(0; 0|t) Z_\eta(0; 0|t)}, \tag{4.1}$$

where Z_η is the partition function 2.6 of a single polymer. A proof for this formula is given in the Appendix A.5. In the free case, substituting $Z_{\eta \equiv 0}$ with the propagator 2.3, the integral at the numerator of 4.1 is solvable, giving

$$P(\tau) = \frac{\sqrt{t}}{2\sqrt{\pi}\sqrt{t-\tau}\tau^{3/2}} = \frac{1}{t^{3/2}} f(q), \tag{4.2}$$

where we have defined the new variable $q = 1 - \frac{\tau}{t}$, so that $q \in]0, 1[$, and the function

$$f(q) = \frac{\sqrt{t}}{2\sqrt{\pi}\sqrt{q}(1-q)^{3/2}} = \begin{cases} \sim q^{-\frac{1}{2}} \text{ if } q \to 0^+ \\ \sim (1-q)^{-\frac{3}{2}} \text{ if } q \to 1^- \end{cases}. \tag{4.3}$$

The limit $q \to 0$ corresponds to two polymers that cross for the first time near the end, while in the limit $q \to 1$ two polymers cross at the very beginning. If we consider two ground states in a disordered medium, qt nearly coincides with the length of the overlap between the two ground states, since, after they cross for the first time, they start to

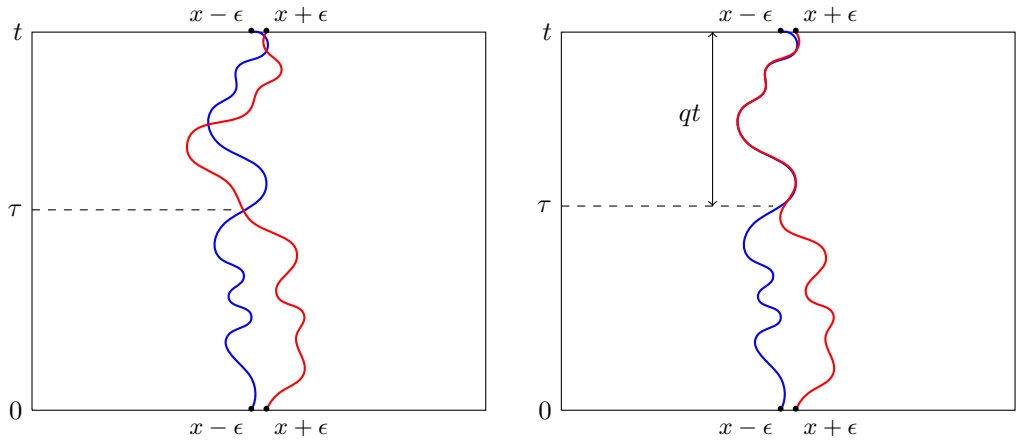

Figure 4.1: Comparison between free directed polymers (on the left), that have no interaction even after the first crossing, and ground states in disordered media (on the right), that present overlap after the first crossing.

follow the same path until the end (see Figure 4.1).

We verify numerically the validity of Equation 4.2 for both free polymers and ground states in disordered media. In practice, we used the same procedure for the creation of a couple of polymer with near initial and ending points adopted for calculating the non-crossing probability and described at Section 3.3, but instead of counting whether a couple cross or not, we measure the time at which the first crossing occur; in particular, if two polymers avoid each other, then $q = 0$. We then plot in a histogram the values of the rescaled first-crossing times $1 - q = \tau/t$ collected, obtaining the plots shown in Figures 4.2 and 4.3. Both the asymptotic trends predicted by Equation 4.2 occur for both free directed polymer and ground states, as well as the scale-free behaviour for $q \to 0$, corresponding to the same behaviour already discussed for the non-crossing probability.

Possible developments of this work should consist in finding an analytical solution for Equation 4.1 valid in presence of disorder, and extending the study for higher dimensions. At the moment results are known only in mean field for Caley tree geometry [34,35]. At the thermodynamic limit $t \to \infty$ and finite temperature T, one expects the validity of the one step replica symmetry breaking:

$$P(q,T) = (1-T)\delta(q) + T\delta(1-q) \tag{4.4}$$

Very recently the same quantity has been computed at finite t [36–38]. It will be then very interesting to study the behaviour of this quantities in finite dimension.

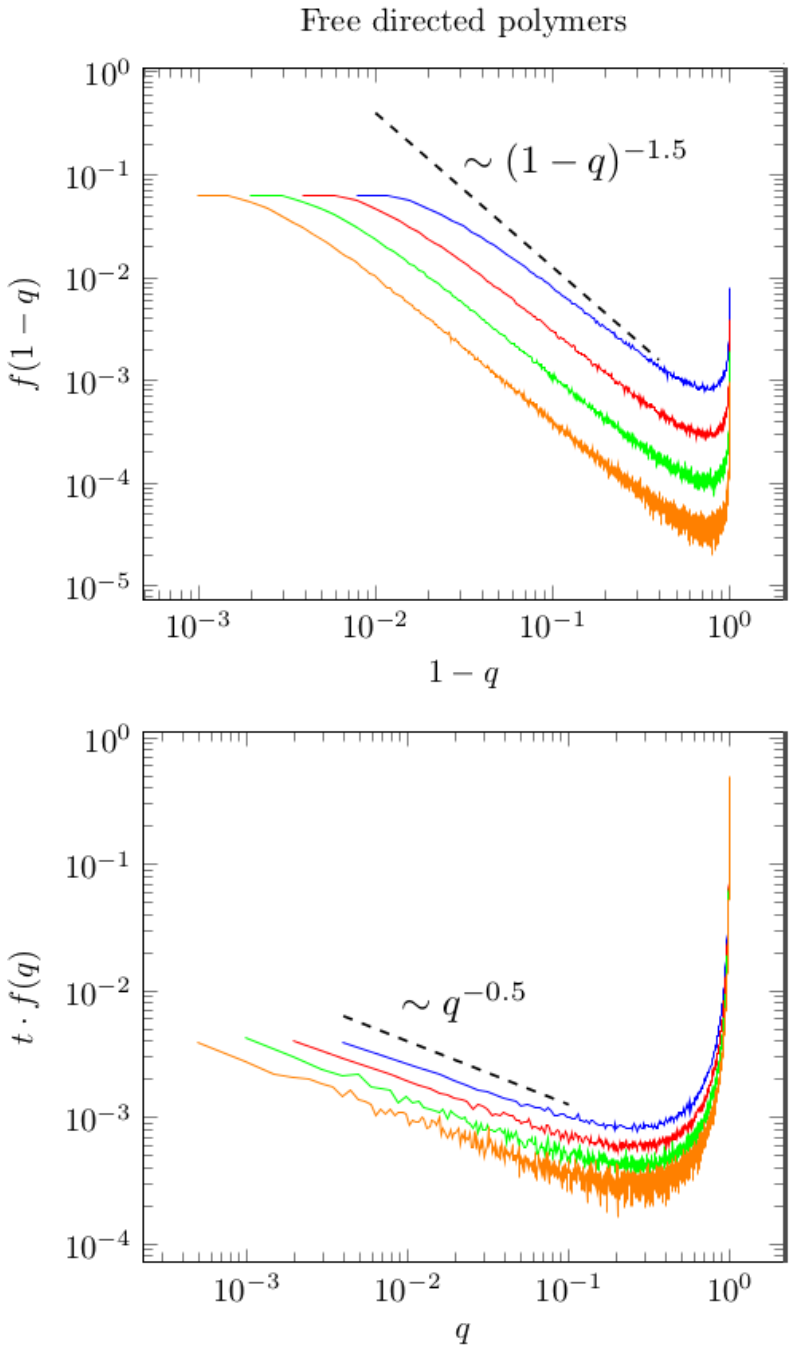

Figure 4.2: Plot of the functions $f(1-q)$ and $t \cdot f(q)$ in $d = 1$ for the free case, obtained for $t = 2^n$, $n = 8, 9, 10, 11$, indicated respectively in blue, red, green and yellow. For every t, 10^6 values were sampled.

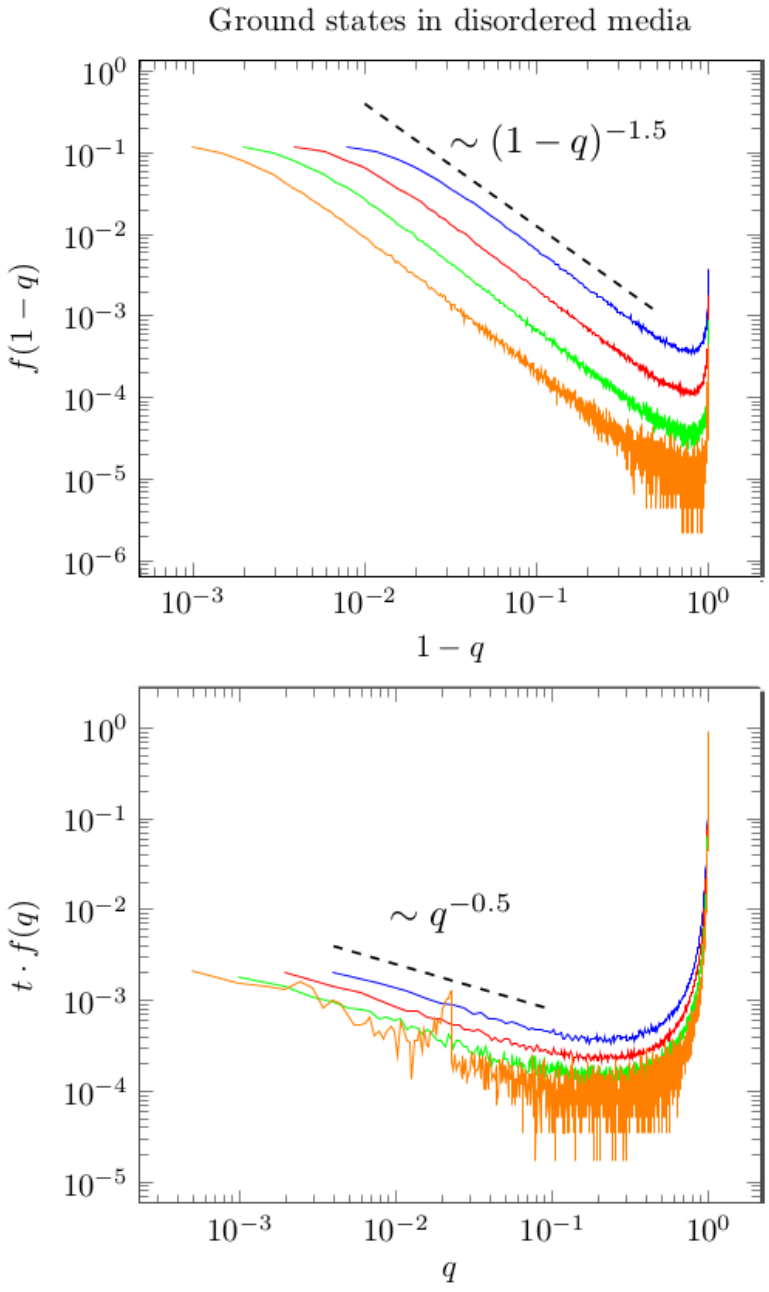

Figure 4.3: Plot of the functions $f(1-q)$ and $t \cdot f(q)$ in $d = 1$ for the disordered case, obtained for $t = 2^n$, $n = 8, 9, 10, 11$, indicated respectively in blue, red, green and yellow. For $n = 8, 9, 10$, 10^6 values were sampled, while $\sim 5 \cdot 10^5$ values were sampled for $n = 11$.

Appendix A

Appendix

A.1 Method of images

In this Appendix we report a proof for Eq. 2.9, valid in $d = 1$ dimension, using the method of images. Choose a couple of paths, that we can call $x_{AA}(t)$ and $x_{BB}(t)$, that present at least one intersection, and at the time of the last cross interchange the label of the two paths (as shown in Figure A.1). In this way a new couple of paths, that we call $x_{AB}(t)$ and $x_{BA}(t)$, is obtained, for which in particular the final endpoints y_A, y_B are exchanged. In a non-rigorous way we can write the partition functions

$$Z_\eta(x_A, x_B; y_A, y_B|t) = \sum_\alpha e^{-E[\alpha]} = \sum_{\alpha'} e^{-E[\alpha']} + \sum_{\alpha''} e^{-E[\alpha'']} \tag{A.1a}$$

$$Z_\eta(x_A, x_B; y_B, y_A|t) = \sum_\beta e^{-E[\beta]} \tag{A.1b}$$

where α labels any pair of original polymers that may presents at least one intersection (α') or no intersections at all (α''), while β labels any pair of polymers with the final parts exchanged. This interchange technique shows that there is a one-to-one correspondence between the ensemble of the pairs of paths type α' and the ensemble of the pairs of paths type β.
Moreover, the energy of a pair of type α' is the same of the pair of its correspondent of type β. In fact the energy of a pair of kind α', for example, is the sum of the energy of

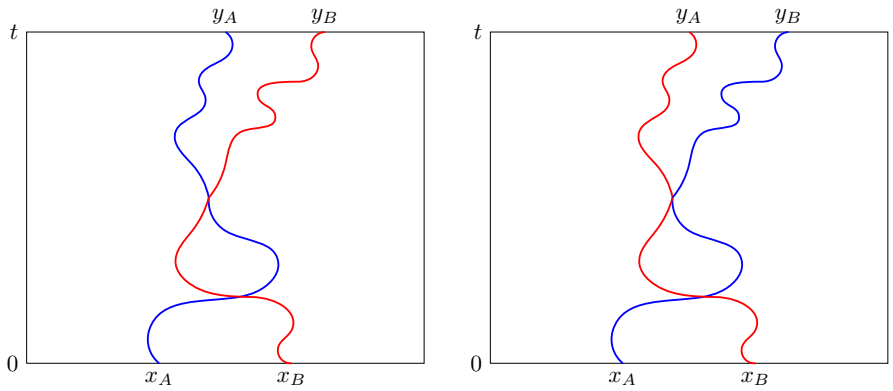

Figure A.1: Left: Two directed polymers in $d = 1$ (one going from x_A to y_A, the other from x_B to y_B) intersecting at least once. Right: Two directed polymer with the same statistical weight but exchanged ends.

the two original polymers,

$$\begin{aligned} E[\alpha'] &= E[x_{AA}(t)] + E[x_{BB}(t)] \\ &= \int_0^t d\tau \left[\frac{1}{4D} \left(\frac{dx_{AA}}{d\tau} \right)^2 + \eta(x_{AA}(\tau), \tau) + \frac{1}{4D} \left(\frac{dx_{BB}}{d\tau} \right)^2 + \eta(x_{BB}(\tau), \tau) \right] \end{aligned} \tag{A.2}$$

if we approximate the derivative as a ratio of discrete increments $\frac{\mathrm{d}x}{\mathrm{d}\tau} \simeq \frac{(\tau+\mathrm{d}\tau)-x(\tau+\mathrm{d}\tau)}{\mathrm{d}\tau}$, we get

$$\begin{aligned} E[\alpha'] = \int_0^t d\tau \, \frac{1}{4D} \left(\frac{x_{AA}(\tau + d\tau) - x_{AA}(\tau)}{d\tau} \right)^2 + \eta(x_{AA}(\tau), \tau) + \\ + \frac{1}{4D} \left(\frac{x_{BB}(\tau + d\tau) - x_{BB}(\tau)}{d\tau} \right)^2 + \eta(x_{BB}(\tau), \tau) \end{aligned} \tag{A.3}$$

since all the quantities in the integrals occur for both the pairs of polymers, we can perform the label change $AA,\ BB \to AB,\ BA$, so that we find the sum of the energy of the polymers with the final parts exchanged:

$$\begin{aligned} E[\alpha'] = \int_0^t d\tau \, \frac{1}{4D} \left(\frac{x_{AB}(\tau + d\tau) - x_{AB}(\tau)}{d\tau} \right)^2 + \eta(x_{AB}(\tau), \tau) + \\ + \frac{1}{4D} \left(\frac{x_{BA}(\tau + d\tau) - x_{BA}(\tau)}{d\tau} \right)^2 + \eta(x_{BA}(\tau), \tau) = \\ = E[x_{AB}(t)] + E[x_{BA}(t)] = E[\beta]; \end{aligned} \tag{A.4}$$

This implies that, for every α', $e^{-E[\alpha']} = e^{-E[\beta]}$, and the non-crossing probability becomes

$$p_\eta(x_A, x_B; y_A, y_B|t) = 1 - \frac{\sum_{\alpha'} e^{-E[\alpha']}}{\sum_\alpha e^{-E[\alpha]}} = 1 - \frac{\sum_\beta e^{-E[\beta]}}{\sum_\alpha e^{-E[\alpha]}} = 1 - \frac{Z_\eta(x_A, x_B; y_B, y_A|t)}{Z_\eta(x_A, x_B; y_A, y_B|t)}, \tag{A.5}$$

giving exactly Eq. 2.9.
Unfortunately, the expression (2.9) is not valid for higher dimensions, e.g. $d = 2$, because, once the final endpoints y_1 and y_2 are exchanged, the two polymers are not obliged to cross, so there is not a one-to-one correspondence between the ensemble of pairs of polymers with at least one intersection and the ensemble of pairs of polymers with y_1 and y_2 exchanged (i.e. the pairs of paths with at least one intersection are less than the pairs of paths with y_1 and y_2 exchanged).

A.2 Laplace transform of First passage probability

Consider the partition function $F(\vec{x} - \vec{x}_0, t)$ of a DP that, starting from $\vec{x}$, arrives at $\vec{x}_0$ for the first time in $[t, t + dt]$. We show we can write its Laplace transform $\hat{F}(\vec{x} - \vec{x}_0, s)$ as a function of the Laplace transform $\hat{G}(\vec{x} - \vec{x}_0, s)$ of the partition function $G(\vec{x} - \vec{x}_0, t)$ of a generic DP going from $\vec{x}$ to $\vec{x}_0$ after a time t. It is convenient to analyze first the case $\vec{x} = \vec{x}_0$, for which the DP starts and ends at the same point $\vec{x}$, and then $\vec{x} \neq \vec{x}_0$.

- **Case $\vec{x} = \vec{x}_0$.** The partition function $G(\vec{0}, t)$ of a generic DP that starts and ends at the same point $\vec{x}$ after a time t can be considered as a sum of different contributes:
  - At $t = 0$ we get the Dirac delta $\delta(t)$;
  - When $t \neq 0$ and the polymer never comes back at $\vec{x}$ before t, we have $F(0, t)$ by definition;
  - If the polymer comes back once to $\vec{x}$ at a generic time $t_1 < t$, the partition function for this specific case is the integral of $F(\vec{0}, t - t_1)F(\vec{0}, t_1)$ in t_1;
  - All the other cases for which the polymer comes back n times at $\vec{x}$, with $n \in \mathbb{N}$, before t;

We can thus write the partition function $G(0,t)$ as the following sum:

$$\begin{aligned} G(\vec{0},t) = \delta(t) + F(\vec{0},t) + \int_0^t dt_1\, F(\vec{0},t-t_1)F(\vec{0},t_1) + \\ + \int_0^t \int_0^t dt_1\, dt_2\, F(\vec{0},t-t_2)F(\vec{0},t_2-t_1)F(\vec{0},t_1) + \ldots; \end{aligned} \tag{A.6}$$

taking the Laplace transform of both members, since the Laplace transform of a convolution of n function is the product of the Laplace transform of these n functions, we have

$$\begin{aligned} \hat{G}(\vec{0},s) &= 1 + \hat{F}(\vec{0},s) + \hat{F}^{\,2}(\vec{0},s) + \hat{F}^{\,3}(\vec{0},s) + \ldots \\ &= \sum_{n=0}^{+\infty} \hat{F}^{\,n}(\vec{0},s) = \frac{1}{1-\hat{F}(\vec{0},s)} \end{aligned} \tag{A.7}$$

and finally inverting the expression

$$\hat{F}(\vec{0},s) = 1 - \frac{1}{\hat{G}(\vec{0},s)}. \tag{A.8}$$

- **Case $\vec{x} \neq \vec{x}_{\mathbf{o}}$.** Similarly to the previous case, we can write the partition function of a generic DP that goes from $\vec{x}$ to $\vec{x}$ as a sum of different contributes (obviously, the case $t = 0$ is not included now)

  - The case for which the polymer never goes to $\vec{x}$ before t, that is $F(\vec{x}-\vec{x}_0,t)$ by definition;

  - The case in which the polymer goes once to $\vec{x}$ at a generic time $t_1 < t$, for which the partition function is the integral of $F(\vec{x}-\vec{x}_0,t-t_1)F(\vec{0},t_1)$ in t_1;

  - All the other cases for which the polymer comes back n times, with $n \in \mathbb{N}$, at $\vec{x}$ before t;

  Calling $\Delta\vec{x} = \vec{x} - \vec{x}_0$, we have

$$\begin{aligned} G(\Delta\vec{x},t) = F(\Delta\vec{x},t) + \int_0^t dt_1\, F(\Delta\vec{x},t-t_1)F(\vec{0},t_1) + \\ + \int_0^t \int_0^t dt_1\, dt_2\, F(\Delta\vec{x},t-t_2)F(\vec{0},t_2-t_1)F(\vec{0},t_1) + \\ + \ldots \end{aligned} \tag{A.9}$$

taking the Laplace transform of both members

$$\begin{aligned}\hat{G}(\Delta\vec{x},s) &= \hat{F}(\Delta\vec{x},s) + \hat{F}(\Delta\vec{x},s)\hat{F}(\vec{0},s) + \hat{F}(\Delta\vec{x},s)\hat{F}^2(\vec{0},s) + \dots \\ &= \hat{F}(\Delta\vec{x},s)\sum_{n=0}^{+\infty}\hat{F}^{\,n}(\vec{0},s) = \frac{\hat{F}(\Delta\vec{x},s)}{1-\hat{F}(\vec{0},s)} = \hat{F}(\Delta\vec{x},s)\hat{G}(\vec{0},s)\end{aligned} \tag{A.10}$$

and finally

$$\hat{F}(\Delta\vec{x},s) = \frac{\hat{G}(\Delta\vec{x},s)}{\hat{G}(\vec{0},s)}. \tag{A.11}$$

which is equivalent to Eq. 2.24 of the main text.

Summarizing these results:

$$\hat{F}(\vec{x},s) = \begin{cases} 1 - \frac{1}{\hat{G}(\vec{0},s)} \text{ if } \vec{x} = 0 \\ \frac{\hat{G}(\vec{x},s)}{\hat{G}(\vec{0},s)} \text{ if } \vec{x} \neq 0 \end{cases} \tag{A.12}$$

A.3 Non-crossing probability for near-coinciding endpoints

If we consider the non-crossing probability 2.9 obtained for $d = 1$ from the method of images

$$p_\eta(x_A, x_B; y_A, y_B|t) = 1 - \frac{Z_\eta(x_B; y_A|t)Z_\eta(x_A; y_B|t)}{Z_\eta(x_A; y_A|t)Z_\eta(x_B; y_B|t)}, \tag{A.13}$$

from the definition of $p_\eta(t)$ provided by 2.44 we have

$$p_\eta(t) := \lim_{\epsilon\to 0}\frac{p_\eta(-\epsilon,\epsilon;-\epsilon,\epsilon|t)}{4\epsilon^2} = \lim_{\epsilon\to 0}\frac{1}{4\epsilon^2}\left(1 - \frac{Z_\eta(\epsilon,-\epsilon)Z_\eta(-\epsilon,\epsilon)}{Z_\eta(-\epsilon,-\epsilon)Z_\eta(\epsilon,\epsilon)}\right). \tag{A.14}$$

On the other hand, using the definition of derivative and the properties of the logarithm:

$$\begin{aligned}
\partial_x\partial_y \log Z(x;y|t)|_{\substack{x=0\\y=0}} &= \partial_x \lim_{\epsilon\to 0} \frac{1}{2\epsilon} \left(\log Z_\eta(x,y+\epsilon) - \log Z_\eta(x,y-\epsilon)\right)|_{\substack{x=0\\y=0}} \\
&= \partial_x \lim_{\epsilon\to 0^+} \frac{1}{2\epsilon} \frac{\log Z_\eta(x,y+\epsilon)}{Z_\eta(x,y-\epsilon)}|_{\substack{x=0\\y=0}} \\
&= \lim_{\epsilon\to 0} \frac{1}{4\epsilon^2} \left(\log \frac{Z(x+\epsilon,y+\epsilon)}{Z(x+\epsilon,y-\epsilon)} - \log \frac{Z(x-\epsilon,y+\epsilon)}{Z(x-\epsilon,y-\epsilon)}\right)|_{\substack{x=0\\y=0}} \\
&= \lim_{\epsilon\to 0} \frac{1}{4\epsilon^2} \log \frac{Z(x+\epsilon,y+\epsilon)Z(x-\epsilon,y-\epsilon)}{Z(x+\epsilon,y-\epsilon)Z(x-\epsilon,y+\epsilon)}|_{\substack{x=0\\y=0}} \\
&= \lim_{\epsilon\to 0} \frac{1}{4\epsilon^2} \log \frac{Z(\epsilon,\epsilon)Z(-\epsilon,-\epsilon)}{Z(\epsilon,-\epsilon)Z(-\epsilon,\epsilon)}
\end{aligned} \tag{A.15}$$

Since the argument of the log in the last member of A.15 tends to 1 from left as $\epsilon \to 0^+$, using the approximation $\log x \underset{x\to 1^-}{\approx} 1-x$ we obtain

$$\partial_x\partial_y \log Z(x;y|t)|_{\substack{x=0\\y=0}} = \lim_{\epsilon\to 0} \frac{1}{4\epsilon^2} \left(1 - \frac{Z_\eta(\epsilon,-\epsilon)Z_\eta(-\epsilon,\epsilon)}{Z_\eta(-\epsilon,-\epsilon)Z_\eta(\epsilon,\epsilon)}\right), \tag{A.16}$$

so, comparing A.14 and A.16 we finally prove the equality 2.46:

$$\lim_{\epsilon\to 0} \frac{p_\eta(-\epsilon,\epsilon;-\epsilon,\epsilon|t)}{4\epsilon^2} = \partial_x\partial_y \log Z(x;y|t)|_{\substack{x=0\\y=0}}. \tag{A.17}$$

A.4 Statistical Tilt Symmetry

Consider the generic partition function of a directed polymer in a disordered medium expressed in Equation 2.6, that we report here

$$Z_\eta(\vec{x};\vec{y}|t) = \int_{\vec{x}(0)=\vec{x}}^{\vec{x}(t)=\vec{y}} \mathrm{D}[\vec{x}]\, e^{-\int_0^t \mathrm{d}\tau \left[\frac{1}{4D}\left(\frac{\mathrm{d}\vec{x}}{\mathrm{d}\tau}\right)^2 + \eta(\vec{x}(\tau),\tau)\right]}. \tag{A.18}$$

A path $\vec{x}(\tau)$ goes from $\vec{x}$ to $\vec{y}$; we can introduce the tilted path $\vec{u}(\tau)$ that starts and ends at the same point $\vec{0}$

$$\vec{u}(\tau) := \vec{x}(\tau) - \frac{(\vec{y}-\vec{x})\tau}{t} - \vec{x}; \tag{A.19}$$

in this way $\vec{u}(0) = \vec{u}(t) = \vec{0}$. Therefore, deriving both members with respect to τ

$$\begin{aligned} \dot{\vec{u}}(\tau) &= \dot{\vec{x}}(\tau) - \frac{\vec{y}-\vec{x}}{t} \implies \\ \dot{x}^2(\tau) &= \dot{u}^2(\tau) + \left(\frac{\vec{y}-\vec{x}}{t}\right)^2 + \frac{2\dot{\vec{u}}(\vec{y}-\vec{x})}{t} \end{aligned} \tag{A.20}$$

Observing then that the Jacobian of the variable change is 1, we have

$$\int_0^t d\tau \left[\frac{\dot{x}^2(\tau)}{4D} + \eta(\vec{x}(\tau),\tau)\right] = \frac{(\vec{y}-\vec{x})^2}{4Dt} + \int_0^t d\tau \left[\frac{\dot{u}^2(\tau)}{4D} + \tilde{\eta}(\vec{u}(\tau),\tau)\right] \tag{A.21}$$

where we have the tilted disorder

$$\tilde{\eta}(\vec{u},\tau) = \eta(\vec{u} - \frac{(\vec{y}-\vec{x})\tau}{t} - \vec{x},\tau); \tag{A.22}$$

In this way $Z_\eta(\vec{x};\vec{y}|t)$ becomes

$$\begin{aligned} Z_\eta(\vec{x};\vec{y}|t) &= e^{-\frac{(\vec{y}-\vec{x})^2}{4Dt}} Z_{\tilde{\eta}}(\vec{0};\vec{0}|t) \implies \\ \log Z_\eta(\vec{x};\vec{y}|t) &= -\frac{(\vec{y}-\vec{x})^2}{4Dt} + \log Z_{\tilde{\eta}}(\vec{0};\vec{0}|t). \end{aligned} \tag{A.23}$$

In general η and $\tilde{\eta}$ are different realizations of the disorder and a dangerous x, y dependence is hidden is $\tilde{\eta}$. But if we determine the correlation of the tilted disorder landscape we get

$$\begin{aligned} \overline{\tilde{\eta}(\vec{u},\tau)\tilde{\eta}(\vec{u}\,',\tau')} &= \overline{\tilde{\eta}(\vec{u}+\tau(\vec{y}-\vec{x})/t+\vec{x},\tau)\tilde{\eta}(\vec{u}\,'+\tau'(\vec{y}-\vec{x})/t+\vec{x},\tau')} \\ &= \delta^{(d)}\left(\vec{u}-\vec{u}\,' + \frac{\vec{y}-\vec{x}}{t}(\tau-\tau')\right)\delta(\tau-\tau') \\ &= \delta^{(d)}(\vec{u}-\vec{u}\,')\delta(\tau-\tau'); \end{aligned} \tag{A.24}$$

namely the correlation of the original η, meaning that $\tilde{\eta}$ has the same distribution of η. Thus averaging both members of A.23 over all realizations of the disorder, we finally get

$$\begin{aligned} \overline{\log Z_\eta(\vec{x};\vec{y}|t)} &= -\frac{(\vec{y}-\vec{x})^2}{4Dt} + \overline{\log Z_{\tilde{\eta}}(\vec{0};\vec{0}|t)}. \\ &= -\frac{(\vec{y}-\vec{x})^2}{4Dt} + \underbrace{\overline{\log Z_\eta(\vec{0};\vec{0}|t)}}_{=:f(t)}. \end{aligned} \tag{A.25}$$

with $f(t)$ independent of x and y as in Equation 2.45.

A.5 PDF of first-crossing time

The probability density that two directed polymers with near-coinciding endpoints cross for the first time at τ could be written, for a fixed realization of the disorder η, as

$$P(\tau) = \lim_{\epsilon \to 0} \frac{\int_{-\infty}^{+\infty} dz\, \tilde{Z}_\eta(\epsilon, -\epsilon; z+\epsilon, z-\epsilon|\tau)\, Z_\eta(z+\epsilon; \epsilon|t-\tau)\, Z_\eta(z-\epsilon; -\epsilon|t-\tau)}{Z_\eta(\epsilon; \epsilon|t) Z_\eta(-\epsilon; -\epsilon|t)}. \tag{A.26}$$

where Z_η is the single polymer partition function, while $\tilde{Z}_\eta$ the partition function of a pair of directed polymers that never intersect before τ. The integrating function at the numerator of Equation A.26 takes then into account all the couples of polymers, starting respectively at $-\epsilon$ and ϵ and ending at the same point, that cross (more precisely, that occur at a distance 2ϵ) for the first time at z; the numerator is instead the partition function of all polymers with the same starting and ending points. Thanks to the method of images valid in $d = 1$, we can write $\tilde{Z}_\eta$ as the partition function of all polymers minus the one with $x + \epsilon$ and $x - \epsilon$ exchanged:

$$\tilde{Z}_\eta(\epsilon, -\epsilon; z+\epsilon, z-\epsilon|\tau) = Z_\eta(\epsilon, x+\epsilon|\tau) Z_\eta(-\epsilon, x-\epsilon|\tau) - Z_\eta(\epsilon, x-\epsilon|\tau) Z_\eta(-\epsilon, x+\epsilon|\tau). \tag{A.27}$$

Defining the function

$$Z_\eta^+(z, \tau) = \lim_{\epsilon \to 0} \tilde{Z}_\eta(\epsilon, -\epsilon; z+\epsilon, z-\epsilon|\tau), \tag{A.28}$$

using the definition of derivative and the properties of logarithm we get

$$\begin{aligned} Z_\eta^+(z, \tau) &= \lim_{\epsilon \to 0} [Z_\eta(\epsilon, x+\epsilon|\tau) Z_\eta(-\epsilon, x-\epsilon|\tau) - Z_\eta(\epsilon, x-\epsilon|\tau) Z_\eta(-\epsilon, x+\epsilon|\tau)] \\ &= \partial_x Z_\eta(x, z|\tau)|_{x=0} \partial_y Z_\eta(x, y|\tau)|_{y=z} - Z_\eta(x, y|\tau) \partial_x \partial_y Z_\eta(x, y|\tau)|_{\substack{x=0 \\ y=z}} \\ &= Z_\eta^2(0, z|\tau) \partial_x \partial_y \log Z_\eta(x; y|\tau)|_{\substack{x=0 \\ y=z}}. \end{aligned} \tag{A.29}$$

Substituting into Eq. A.26 we obtain

$$\begin{aligned} P(\tau) &= \lim_{\epsilon \to 0} \frac{\int_{-\infty}^{+\infty} dz\, Z_\eta^2(0; z|\tau)\, Z_\eta(z+\epsilon; \epsilon|t-\tau) Z_\eta(z-\epsilon; -\epsilon|t-\tau)\, \partial_x \partial_y \log Z_\eta(x; y|\tau)|_{x=0, y=z}}{Z_\eta(\epsilon; \epsilon|t) Z_\eta(-\epsilon; -\epsilon|t)}, \\ &= \frac{\int_{-\infty}^{+\infty} dz\, Z_\eta^2(0; z|\tau)\, Z_\eta^2(z; 0|t-\tau)\, \partial_x \partial_y \log Z_\eta(x; y|\tau)|_{x=0, y=z}}{Z_\eta(0; 0|t) Z_\eta(0; 0|t)}, \end{aligned} \tag{A.30}$$

returning exactly Equation 4.1.

Resources

The programs developed for the numerical simulations in Chapter 3 and 4 are written in C++ and Python languages. All the main codes can be found at `https://github.com/FedericoLanza/MscThesis`. These codes are licensed under the GNU General Public License version 3.0 (`https://opensource.org/licenses/GPL-3.0`). The simulations have been run on the last version of the codes; the dates are reported in the comments at the beginning of the files. All the libraries needed for the deployment of every algorithm are currently already being integrated into the C++ and Python Standard Libraries.

Bibliography

[1] H. Darcy, *Les fontaines publiques de la ville de Dijon: exposition et application des principes à suivre et des formules à employer dans les questions de distribution d'eau* (Victor Dalmont, 1856).

[2] A. C. Barbati, J. Desroches, A. Robisson, and G. H. McKinley, "Complex fluids and hydraulic fracturing", Annual Review of Chemical and Biomolecular Engineering

[3] R. P. W. Soyka, A. López, C. Persson, L. Cristofolinic, S. J. Fergusona, "Numerical description and experimental validation of a rheology model for non-Newtonian fluid flow in cancellous bone", Journal of the Mechanical Behavior of Biomedical Materials **27**, 43-53 (2013)

[4] T. Al-Fariss, K. L. Pinder, "Flow through porous media of a shear-thinning liquid with yield stress", Can. J. Chem. Eng. **65**, 391 (1987).

[5] T. Chevalier, C. Chevalier,, X. Clain, J.C. Dupla, J. Canou, S. Rodts, P. Coussot, "Darcy's law for yield stress fluid flowing through a porous medium", J. Non-Newtonian Fluid Mech. **195**, 57 (2013).

[6] L. Talon and D. Bauer, "On the determination of a generalized Darcy equation for yield-stress fluid in porous media using a Lattice-Boltzmann TRT scheme" Eur. Phys. J. E **36**, 1 (2013)

[7] L. Talon, H. Auradou, M. Pessel, and A. Hansen, "Geometry of optimal path hierarchies", EPL (Europhysics Letters) **103**, 30003 (2013).

[8] T. Chevalier and L. Talon, "Generalization of Darcy's law for Bingham fluids in porous media: From flow-field statistics to the flow-rate regimes", Phys. Rev. E **91**, 023011 (2015).

[9] T. Chevalier and L. Talon, "Moving line model and avalanche statistics of Bingham fluid flow in porous media", Eur. Phys. J. E. **38**, 76 (2015).

[10] P. Forchhemier, "Wasserbewegung durch boden", Z. Ver. Deutsch, Ing. **45**, 1782-1788 (1901).

[11] C. C. Mei and J.-L. Auriault, "The effect of weak inertia on flow through a porous medium", J . Fluid Mech. **222**, 647-663 (1991).

[12] S. Whitaker, "The Forchheimer Equation: A Theoretical Development", Transp. Porous Media **25**, 27 (1996).

[13] I. Fatt et al., "The network model of porous media", Society of Petroleum Engineers (1956). **7**, 415 (2016).

[14] J. Nittmann, G. Daccord, and H. E. Stanley, "Fractal growth of viscous fingers: quantitative characterization of a fluid instability phenomenon", Nature **314**, 141 (1985).

[15] E. C. Bingham, *Fluidity and plasticity*, Vol. 2 (McGraw-Hill, 1922), p. 219.

[16] B. Drossel and M. Kardar, "Phase Ordering and Roughening on Growing Films", Phys. Rev. Lett. **85**, 614 (2000).

[17] C. Liu, A. De Luca, A. Rosso and L. Talon, "Darcy law for yield stress fluid", Phys. Rev. Lett. **122**, 245502 (2019).

[18] A. Hansen and J. Kertész, "Phase Diagram of Optimal Paths", Phys. Rev. Lett. **93**, 040601 (2004).

[19] G. Pólya, "Kombinatorische Anzahlbestimmungen für Gruppen, Graphen und chemische Verbindungen", Acta Math. **68**, 145-254 (1937).

[20] D. A. Huse and C. L. Henley, "Pinning and Roughening of Domain Walls in Ising Systems Due to Random Impurities", Phys. Rev. Lett. **54**, 2708 (1985).

[21] D.A. Huse, C. L. Henley, and D. S. Fisher, "Huse, Henley, and Fisher respond", Phys. Rev. Lett. **55**, 2924 (1985)

[22] M. Kardar and Y.-C. Zhang, "Scaling of Directed Polymers in Random Media", Phys. Rev. Lett. **58**, 2087 (1987).

[23] A. J. McKane and M. A. Moore, "Mechanism for Superuniversal Behavior in Certain Stochastic Systems", Phys. Rev. Lett. **60**, 527 (1988).

[24] T. Hwa and D. S. Fisher, "Anomalous fluctuations of directed polymers in random media", Phys. Rev. B **49**, 3136 (1994).

[25] A. De Luca and P. Le Doussal, "The crossing probability for directed polymers in random media.", Phys. Rev. E **92**, 040102(R) (2015).

[26] A. De Luca and P. Le Doussal, "Crossing probability for directed polymers in random media. II. Exact tail of the distribution", Phys. Rev. E **93**, 032118 (2016).

[27] S. Karlin and J. L. McGregor, "Coincidence Probabilities", Pacific J. Math **9**, 1141 (1959).

[28] W. Feller, *An Introduction to Probability Theory and its Applications, Vol. 1* (John Wiley & Sons Inc., 1957).

[29] S. Redner, "Systems with Spherical Symmetry", in *A Guide to First-Passage Processes* (Cambridge University Press, 2007), pp. 218-221.

[30] B. D. Hughes, *Random Walks and Random Environments: Volume 1: Random Walks* (Clarendon Press, 1995)

[31] T. E. Hull and C. Froese, "Asymptotic behaviour of the inverse of a Laplace Transform", Canadian Journal of Mathematics **7**, 116-125 (1955).

[32] E. W. Dijkstra, "A note on two problems in connexion with graphs", Numerische Mathematik **1**, 269-271 (1959)

[33] M. T. Goodrich, R. Tamassia, *Data Structures and Algorithms in Java* (Wiley, 2005), pp. 849-857

[34] H. A. Bethe, "Statistical Theory of Superlattices", Proc. Roy. Soc. Lond. A. **150**, 552–575 (1935).

[35] B. Derrida and H. Spohn, "Polymers on Disordered Trees, Spin Glasses, and Traveling Waves", Journal of Statistical Physics **51**, Nos. 5/6 (1988)

[36] G. Parisi, "A Conjecture on random bipartite matching", ArXiv (2018)

[37] B. Derrida and P. Mottishaw, "On the genealogy of branching random walks and of directed polymers", EPL (Europhysics Letters) **115**, 40005 (2016).

[38] X. Cao, A. Rosso, R. Santachiara, and P. Le Doussal, "Liouville Field Theory and Log-Correlated Random Energy Models", Phys. Rev. Lett. **118**, 090601 (2017)

Acknowledgements

I did all my thesis work at Laboratoire de Physique Théorique et Modèles statistiques of Université Paris-Sud, at Orsay in France. I would like to sincerely thank my supervisor Alberto Rosso for having helped me in every part of the work, monitoring my progress constantly and answering to literally all my doubts. I would like to thank also all the members of the laboratory for making me feel a part of it during those months.

I dedicate all my gratitude to my family, for having supported me in all my choices.
Thanks by heart to my friends Elisabetta, Michela and Piero, with whom I've shared joyful moments, and also endless afternoons of study.
A special thanks to all my friends from university who have walked beside me, even for a part, along this incredible journey that started from the first year of Bachelor in Physics and is going to finish now.
And thanks also to me, whom I wish happiness and suggest never stop learning.